PONTIFICIA UNIVERSIDAD CATÓLICA DEL PERÚ

ESCUELA DE POSGRADO

DESIGN AND IMPLEMENTATION OF A BRISTLE BOT SWARM SYSTEM

Author:

Ing. Juan Edmundo Pozo Fortunić

Advisor:

Dr.-Ing. Felix Becker, from TU Ilmenau

Responsible Professors:

MSc. Francisco Fabián Cuéllar Córdova, from PUCP

Univ. -Prof. Dr.-Ing. habil. Klaus Zimmermann, from TU Ilmenau

March 2016

Ilmenau, Germany

KURZFASSUNG

Die Schwarmrobotik ist ein Wissenschaftsgebiet, das sich auf die Untersuchung und Entwicklung von Robotersystemen fokussiert, die aus einer großen Menge von Einzelrobotern (Agenten) bestehen. Die Agenten interagieren dabei miteinander und erreichen so ein gemeinsames Verhalten. Das Ziel ist die kooperative Erfüllung von Aufgaben und die Überwindung von Hindernissen. Bristlebots sind vibrationsbasierte mobile Roboter. Sie sind durch eine geringe Größe, eine hohe Geschwindigkeit, einen einfachen Aufbau und geringe Kosten für Produktion und Betrieb gekennzeichnet, was vorteilhafte Eigenschaften für Agenten in einem Roboterschwarm darstellen. Die in der Literatur bisher vorgestellten Systeme besitzen keine Steuerung oder arbeiten mit zwei oder mehr Antrieben.

An dieser Stelle setzt die vorliegende Masterarbeit an. Ziel ist die Entwicklung eines Bristlebot-basierten Agenten für einen miniaturisierten Roboterschwarm. Der Roboter soll ein Lokomotions-, Sensor-, Informationsverarbeitungs-, Kommunikations- und Energiespeicherungssystem besitzen. Neue Beiträge zu Modellierung und Entwicklung von Schwarmrobotern werden geleistet und ein neuartiger Prototyp wird vorgestellt. Der Prototyp wird von einem einzigen Gleichstrommotor angetrieben und benutzt ein Fortbewegungssystem auf Basis von Borsten. Der Systementwurf erfolgte unter den Kriterien einer möglichst geringen Masse, Größe und Komplexität.

Mit dem entwickelten Prototyp wurden Experimente durchgeführt, um seine Bewegungsfähigkeiten zu analysieren. Das System bewegt sich auf leicht gekrümmten Trajektorien vorwärts. Die Richtung der Kurvenfahrt kann durch die Rotationsrichtung des Motors gesteuert werden. Eine Vergrößerung der Drehzahl führt zur Erhöhung der Geschwindigkeit des Roboters. Übersteigt die Drehzahl einen kritischen Wert, invertiert sich das Kurvenverhalten und die translatorische Geschwindigkeit sinkt.

ABSTRACT

Swarm robotics focuses on the study and development of robot systems containing a large number of agents that interact with each other in a collective behaviour in order to achieve tasks or overcome obstacles. Bristlebots are vibration-driven mobile robots. They are characterized by small size, high speed, simple design and low costs for production and application – qualities which are advantageous for agents of swarm robotic systems. However, most studies have been developed over systems with no control or systems with two or more actuators.

The aim of this master thesis is the development of a bristle based robot agent for a swarm robotics microsystem with units for locomotion, sensing, data processing, control, communication and energy storage. New approaches in modelling and development of swarm agents are given, and a robot prototype is presented. The robot is driven by a single DC motor and uses a bristle system to create locomotion. It should be noted, that within the system design, considerations for the size, weight and minimalist architecture are taken.

Experiments are presented and the system's capabilities for displacement, velocity and trajectory generation are analysed. While the parallel velocity maintains a positive magnitude in both motor rotation directions, the rotation speed and transversal velocity of the robot have opposite directions, creating curved trajectories with opposite orientations. In Frequencies up to 210 Hz, the rotation direction of the robot is maintained while the magnitude slightly varies. However, for higher frequencies, the rotation direction of the robot is reversed, maintaining a similar magnitude. The transversal speeds at this frequency range, maintain their direction but are clearly reduced compared to lower frequencies.

.

Para Giacomo y Julieta.

ACKNOWLEDGEMENTS

The current work was made thanks to the support of:

The cooperation between PUCP and TU Ilmenau.

The PUCP Marco Polo Fund, and the DAAD.

Prof. Cuellar and Dr. Felix Becker; for their patience, support, and guidance.

Prof. Zimmermann; for the opportunity and teachings in robotics.

CONTENT INDEX

TABLE INDEX

FIGURE INDEX

Page.

LIST OF SYMBOLS

P_1, P_2	:	Mass points
C	:	Centre of mass
A	:	Actuation point of eccentric mass
m_1, m_2	:	Mass of points P_1, P_2 [kg]
m_e	:	Eccentric mass of the motor [kg]
m	:	Total mass of the robot [kg]
a	:	Distance between C and A [m]
b_1, b_2	:	Distance between C and $P_1$and P_2 [m]
θ	:	Rotation angle [rad]
Ω	:	Angular velocity of motor [rad/s]
g	:	gravity [m/s^2]
$\vec{N}_1, \vec{N}_2$	:	Normal forces [N]
$\vec{F}_{R1}, \vec{F}_{R2}$	:	Coulomb dry friction forces [N]
$\vec{F}_{A1}, \vec{F}_{A2}$	:	Actuation forces [N]
ω	:	Rotation of the robot [rad/s]
$\vec{v}_p$	:	Parallel velocity of the robot [mm/s]
$\vec{v}_t$	:	Transversal velocity of the robot [mm/s]
H	:	Header marker
$\overrightarrow{r_C}$	:	Position of C [mm]
$\overrightarrow{r_{\mathrm{H}}}$	:	Position of H [mm]
$\overrightarrow{r_{CH}}$	:	Relative position of H from C [mm]

LIST OF ABBREVIATIONS

ASIC	:	Application specific integrated circuit
IR	:	Infrared
DC	:	Direct current
PWM	:	Pulse width modulation
PCB	:	Printed circuit board
IrDA	:	Infrared data association
RGB	:	Red green blue
LED	:	Light-emitting diode
CLW	:	Clockwise
CCW	:	Counter clockwise
ADC	:	Analogue to Digital Converter
TWI	:	Two wire interface
Cmd	:	Command
GUI	:	Graphic user interface

CHAPTER I

SWARM ROBOTS AND BRISTLEBOTS

1.1 Introduction

When robotics started, its main field of application became industry, where the first robot manipulators where applied and researched upon. However, since the 1990s, several lines of robotic research have been developed due to evolution of technology, and thus, the research on robot manipulators, mobile robots and biologically inspired robots have significantly increased in the past years [1]. One biologically inspired research branch appears from the observation of certain insects that live in colonies such as: ants, bees, wasps and termites. Despite being complex creatures on their own; the level of complexity achieved by living in colonies is highly superior to one itself, enabling them to overcome larger obstacles or tasks working together [2]. Swarm robotics focuses on the study and development of robot systems containing a large number of agents that interact with each other in a collective behaviour in order to achieve tasks or overcome obstacles. These robot agents overcome their objectives by sensing, processing information individually, communicating with its peers, and actuating all together following a set of simple rules. Their basic modules are: locomotion, communication and sensing, data processing and control, and energy storage and management.

As the difference between the complexity of an insect and its colony capabilities, swarm researchers work to achieve simpler hardware platforms for each robot agent and simpler behavioural algorithms in order to achieve complex objectives as a set. One of the most important modules that define the complexity of an agent is its locomotion module. Several type of actuators, such as: piezoelectric drives, dc motors, vibration motors, coils and magnets; have been used in different configurations (wheels, legs, bristles, etc.) in the development of different micro robots with different locomotion modules [3] [4] [5] [6] [7] [8]. All of these designs use two or more actuators. Bristle based locomotion have shown adequate capabilities for displacement [9]; however, most studies have been developed over systems with no control [10] or systems with two or more actuators. Therefore, to

simplify the architecture of the agent, a one-actuator bristle locomotion system is proposed to study. With a proper electronic control board, a single-actuator bristle-based micro-robot could increase its capabilities to be further developed as a swarm robotic system.

1.2 Objectives

1.2.1 Main objective

Design and implement a micro-robot agent for a swarm system with a single-actuator bristle-based locomotion module, and capabilities for: sensing, communication, velocity control, and trajectory generation.

1.2.2 Specific objectives

- Design and implantation of an electronic module for control, data sensing and processing, communication and power distribution.
- Design and implantation of an exchangeable bristle body
- Design of a programming and control interface for the micro-robot agents on a PC.
- Evaluation of the motion performance of the robot (velocity and trajectory generation)

1.3 State of the Art

1.3.1 Swarm robots

Swarm robotics research is a recent topic. It focuses on the study and development of robot systems containing a large number of agents that interact with each other in a collective behaviour in order to achieve tasks or overcome obstacles. There are three key aspects in the development of a swarm system that defines its capacities: the complexity and physical capabilities of a swarm agent, the communication capabilities for peer-to-peer and collective interaction between agents; and the number of agents in a swarm. The first aspect is approached by hardware development of the agent; the second, the development of novel communication algorithms to enhance collective interaction; and the third, is

embedded within the other two, since adding another agents depends on the fabrication of an agent and the communication limiting capabilities [11].

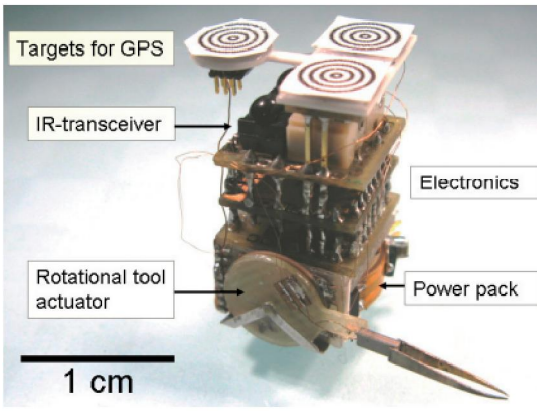

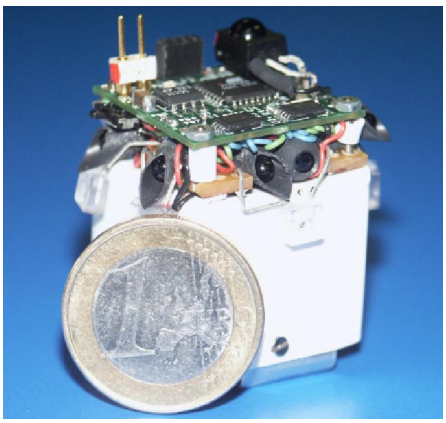

(a) Prototype of MiCRoN and its parts [12] *(b) Prototype of Jasmine [13]*

Figure 1.1 State of the art of micro-robots used in swarm robotics. I

Early developments of micro robots such as Alice [3] and MINIMAN [4] lead to the increase in development of micro-robots and swarm robotics. Casanova et al. developed MiCRoN [5], a swarm robotic system with micro-agents capable of carrying tool, like: a syringe, a gripper or an atomic force microscope (AFM) for task development. MiCRoN possesses a locomotion module, carrier, consisting in a four-piezoelectric-bars configuration that provides three degrees of freedom: transversal and lateral translation, and rotation around the vertical axis. Its manipulator module, rotor, capable of tool-carrying and positioning, is composed of three multilayer piezoelectric bimorph actuators. It includes two targets for Moiré-based positioning [12] and its electronics control module is based on an application specific integrated circuit of their own development with: IrDA communication capabilities, signal generators, a PID controller, and an actuator driver. Its power management module is composed of high voltage operational amplifiers (HVOA) on a power addressing and amplification integrated circuit, a stack of three cell-batteries; and a power-harvesting-coil [14].

Kornienko et al. developed Jasmine [13], an open source hardware and software system oriented to research behavioural algorithms and communication in swarm systems. Jasmine possess a modular sandwich structural design; in which, its modules are connected vertically, one on top of the other, and special modules can be added. On the top layer, the communications module is based on an infrared sensors

array which enables it to communicate with other agents and develop a 360 degree spatial orientation against obstacles. On another layer, the control and data processing unit is based on two microcontrollers: an ATMEGA168 for navigation and sensing; and an ATMEGA88 for locomotion processing. The bottom layer contains the locomotion module, based on a differential wheeled drive using two micro motors; which grants the robot translation and rotation capabilities.

Woern et al. presented the project I-SWARM [6], a micro-robot swarm system with a very small agent (3x3x3 mm^3). Its architecture consists of a flexible printed circuit (FPC) connecting its modules. The locomotion module is based on a three-legged structure that vibrates by a piezoelectric copolymer, enabling translation and rotation. Its control and processing module is based on an 8051 processor with a 10 kB SRAM and no flash memories within an ASIC that can turn on or off its sub-modules to maximize energy efficiency. It possess an IR-based communication and sensing module, and its power module is comprised of solar cells and capacitors to store power [12].

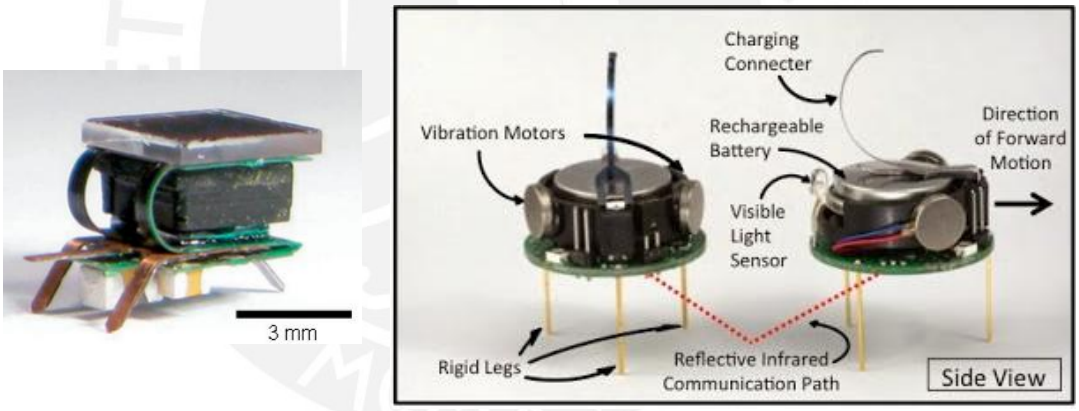

(a) I-SWARM [12] *(b) Kilobot and its parts [7]*

Figure 1.2 State of the art of micro-robots used in swarm robotics. II

Rubenstein et al. developed Kilobot [7], a swarm system oriented to the development of collective behaviour algorithms maintaining a low fabrication cost in its agents. Its locomotion is based on a wheel-less differential drive using two coin-shaped vibro-motors that allows translation and rotation. The control and data processing is based on an ATMEGA328 microcontroller. Its sensing and communications capabilities are based on an isotropic infrared emitter and receiver on the bottom of the robot, where light is reflected on the floor surface to allow a 2D-omnidirectional

communication. Also, a visible light sensor is used for upwards communication through computer vision.

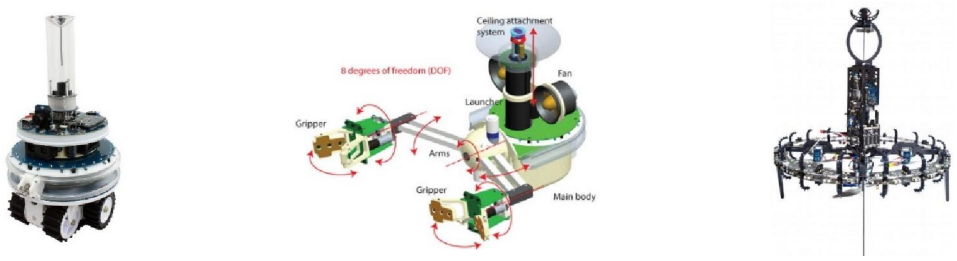

(a) Foot-bot *(b) Hand-bot* *(c) Eye-bot*

Figure 1.3 Swarmanoid types of agents [15]

However, not all swarm systems use micro-robots. The Swarmanoid project, a "Future and Emerging Technologies" project funded by the European commission and lead by Dr. Marco Dorigo, developed a system oriented to the application of swarm robotic techniques into standard-scaled systems [16]. Swarmanoid possess three widely different types of agents called Foot-bot, Hand-bot, and Eye-bot, where their different characteristics enables them to work collectively in a wider range. The Eye-bots, possess an eight-rotor coaxial quadrocopter architecture orientated to sensing and analysing the work ambient from a higher position. The Hand-bots, specialized in object manipulation and vertical displacement between the floor and the ceiling, possess two grippers. The Foot-bots, are mobile robots specialized on displacement on rough terrains, capable of transporting other robots, like the Hand-bot. Their locomotion is based on a two wheeled differential drive. All three type of agents carry a high capacity microprocessor, different arrays of IR and luminous sensors, or cameras for computer vision according to its functions.

1.3.2 Bristle based micro-robots

The locomotion system of these micro-robots are developed using brush-fibres, also known as bristles, as the mechanical interaction between the robot and the surface. The interaction between the system's inertia and the asymmetrical friction forces between the bristles and the floor surface create an asymmetrical translation which results in a displacement in one direction.

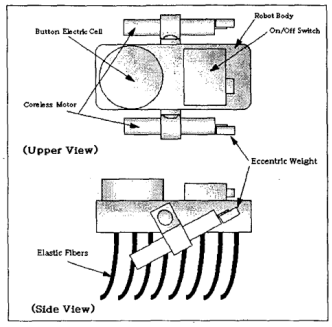

(a) Conceptual view [17]

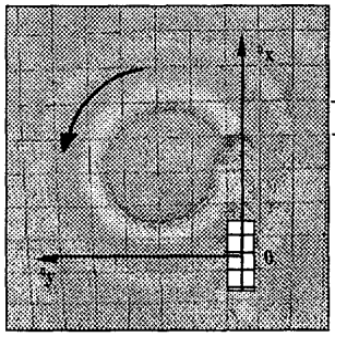

(b) Rotational displacement developed. [18]

Figure 1.4 Bristle-based micro-robot proposed by Ioi

Ioi developed in 1999 a bristle-based micro-robot [17] in order to inspect thin pipes. Its architecture is based on two symmetrically placed vibro-motors, a battery and an on/off switch over and a bristle-based structure. A mathematical model is derived for the translation of the robot using centrifugal forces and modelling the bristles as linear-elastic and viscous materials. An analysis on the displacement and velocity is devolved over the effects of the inclination angle between the vibro-motors and the surface; and, its turning properties controlling the rotational speed of both vibro-motors. Later on, he developed a study [18] to clarify the turning motion of its micro-robot; where, it's shown that circular trajectories can be developed by rotating one of the vibro-motors.

Becker et al. [9], developed a theoretical model of a micro-robot and its prototype to investigate the principle of motion of bristle-based robots. Its architecture is based on two 180^{o}-phased synchronized vibro-motors rotating in opposite directions, a light emitter for positional analysis and an exchangeable bristle base, where different characteristics of the bristles can be selected. Experimental and numerical parameter studies were performed to find dependencies between velocity and the excitation (vibro-motor frequency), the mass, and the bristle design (length, angle, stiffness, etc.), where results show that faster velocities can be obtain with higher frequencies, stiffer bristles with small inclination angles. No steering analysis or control were evaluated; and, the usage of two actuators is still present.

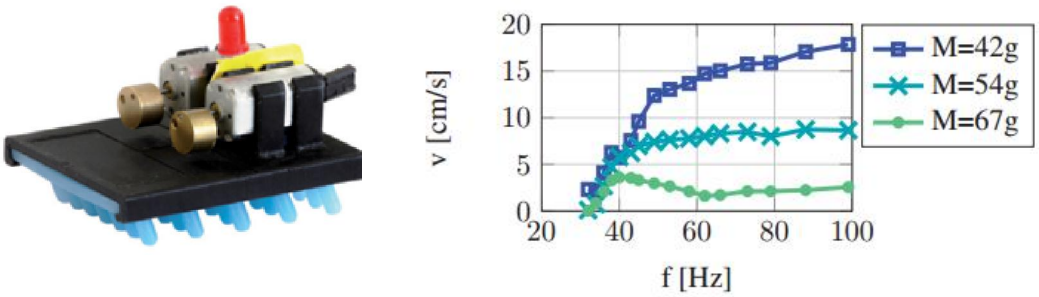

(a) Prototype *(b) Numerical study of the robot speed dependency over frequency and robot mass.*

Figure 1.5 Bristlebot used by Becker et al. [5]

Single-actuator bristle-based micro-robots have grown in recent years as toys. Oskay presented Bristlebot [10], a *do-it-yourself* micro-robot using a vibro-motor, a coin cell battery, and a toothbrush. It was made as a general purpose and entertainment robot for anyone. Innovations First Lab Inc. developed Hexbug Nano [19], an industrialized version of Bristlebot, consisting of a vibro-motor, a coin cell battery, and a plastic casing with elastic bristles. Structures and mazes can be bought from the same company to see the behaviour of the Hexbug on different types of environments.

(a) Bristlebot [10] *(b) Multicolour Hexbug Nanos [19]*

Figure 1.6 Popular and commercial single-motor bristle-based micro-robots.

Lysenko et al. developed a crawling micro-robot Vibro-worm [20] for navigation through pipelines. Its mechanical structure is comprised of a cylindrical body with bristles in all of its surface. Later on, Becker et al. developed a spy bristlebot [21] for pipeline inspection. Its architecture is based on the Vibro-worm structure, a cell phone vibration motor, an accumulator of 220 mAh; and, a spy camera with an

integrated flash disk and USB interface. Since, the trajectory is predefined in pipeline structures, no steering control was developed or analysed for these micro-robot.

Giomi et al. developed and a quantitative study on displacement and velocity over BBot [22] , a one-motor bristlebot swarm. This was performed on a restricted environment to analyse the principle on collective motion in agents with limited sensing capabilities. Their results show that three typical behaviours can occur. These depend on the agents' capabilities to translate and rotate, and the ability to interact with each other and the boundaries and topography of their environment.

As we can see, these micro-robot systems have developed bristle-based locomotion with a single-actuator; however, none of the previous models have developed a trajectory generation study for these type of bristle bots. Neither, a basic control platform with sensing and communication capabilities for a single-actuator bristle-based swarm micro-robot system have been developed.

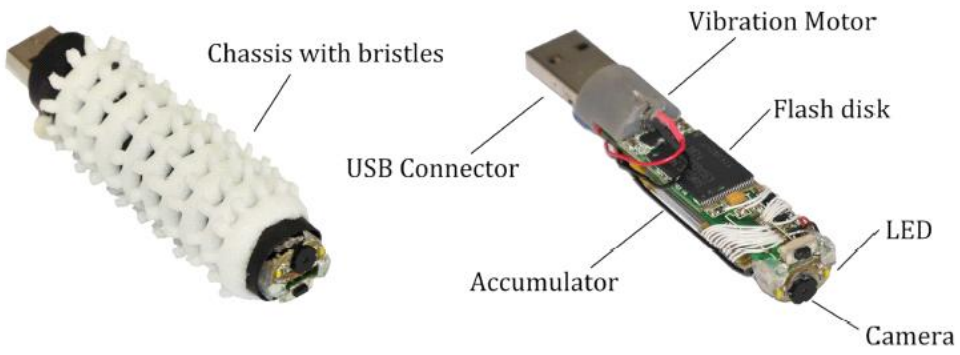

(a) overall system *(b) Internal electronics.*

Figure 1.7 Prototype of the spy bristle bot. [21]

1.4 Preliminary block diagram

Figure 1.8 shows the block diagram of the preliminary swarm robotic system: a Programming and control interface developed on a pc with the appropriate software, and peripherals; and a robot agent, divided into an electronic and mechanical subsystems. The electronic module provides with the necessary modules: control and data processing, communication and sensing, locomotion and power management.

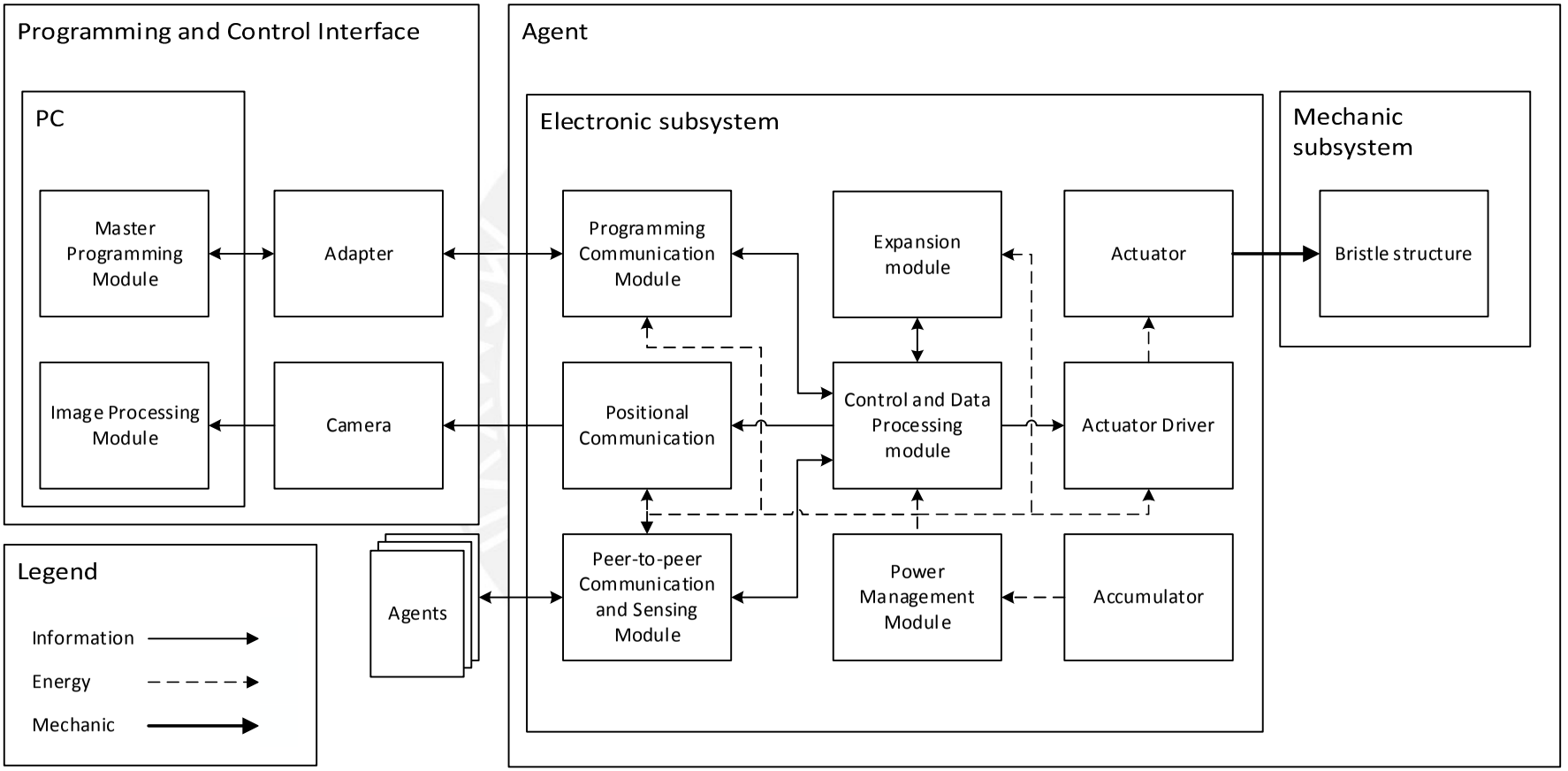

Figure 1.8 Block Diagram of the preliminary system

CHAPTER II

DESIGN OF THE ROBOT AGENT

This chapters exposes the electronic and mechanical designs for a single-actuator bristle-based micro-robot agent for swarm robotics. Its design is based upon the agent section of the preliminary block diagram shown in Figure 1.8.

2.1 Design considerations

Some considerations based on a priori statements and basic elements are given in order to achieve the proposed objectives of this work. These are presented in Table 2-1.

Table 2-1 Design Considerations

Criteria	Specification	Priority
General		
Reproducibility	Design must be reproducible	High
Price	Low	Low
Mechanics		
Size	Maximum: 80x 50x 30 mm^3	High
Weight	Maximum : 50 g	Medium
Bristle-body	Exchangeable	Medium
Bristles	Elastic	High
Actuator	Single vibro-motor	High
Electronics		
Compatibility	Compatible with Arduino [23]	High
Microprocessor	Reprogrammable	High
Communications	Peer-to-peer	High
Communications	Programming	High
Sensing	Environment sensing	Medium
Energy	Internal accumulator	High
Expansion	Able to add expansion boards	High
Soldering and Assembly	Manually	Medium

Developed by the author

2.2 Electronic subsystem

Here are presented the preselected electronic components, selection criteria and designs for the electronic subsystem and its respective modules for the robot agent.

2.2.1 Locomotion module

The electronic actuator and driver of the locomotion subsystem design are explained and selected here. For the mechanical part of the subsystem, please refer to subsection **Error! Reference source not found.**.

2.2.1.1 Actuator

Since the robot agent is a bristle-based system, vibro-motors can be used to develop the locomotion technique; and thus, Table 2-2 shows the preselected motors. Size, vibration amplitude, operating voltage and current, and mounting capabilities were taken in consideration. A 3.0V operating Voltage was preselected given that 3.3V is one of the most typical batteries and IC operating voltage.

Table 2-2 Preselected vibro motors

Model	306-114	304-111	304-100
Body Diameter (mm)	6	4.5	4.4
Full Length (mm)	12.9	14.0	13.2
Rated Operating Voltage (V)	3.0	3.0	3.0
Rated Vibration Speed (RPM)	14 000	15 000	15 000
Typical Rated Operating Current (mA)	57	50	64
Typical Normalized Amplitude (G)	1.15	1.00	1.00
Price (EUR €)	6.14	5.73	6.14

Extracted from [24]

The vibration speeds are similar in all models. Their body diameters and lengths do not vary considerably also; however, a small difference in present in the operating current. Emphasising on the motor price, the model **304-111** is selected.

2.2.1.2 Actuator driver

In order to develop a proper control over a DC vibro-motor, an *H-bridge* configuration circuit and PWM generation is needed. H-Bridge circuits are able to

control the rotation and direction of the motor using two signals, and, with the use of PWM, the motor speed can be controlled. The motor driver specifications should comply with the selected motor characteristics. Table 2-3 shows the preselected drivers and its parameters, extracted from their respective datasheets.

Table 2-3 Preselected motor drivers

Model	DRV8850	DRV8837	DRV8838
Operating supply voltage (V)	2.0~5.5	1.8~7.0	1.8~7.0
Operating Load Voltage (V)	2.0~5.5	0~11.0	0~11.0
Maximum load current (A)	8.0	1.8	1.8
Control Interface	IN-IN	IN-IN	PHASE/ENABLE
Number of Half H-Bridges	2	2	2
Package	24-VQFN	8-WSON	8-WSON
Package Size (mm^2)	5.5 x 3.5	2.0 x 2.0	2.0 x 2.0
Price (EUR €)	1.99	1.30	1.30

All preselected drivers comply with the vibro-motor's specifications; however, given that the package of the DRV8850 is considerably larger and it is more expensive, it is discarded. A PHASE/ENABLE interface allows an easier programming by needing only one PWM signal (ENABLE); however, an IN-IN interface enables the use of the coast and break stages for expanded locomotion research; but, two PWM signals are required. Since, both drivers can be used and have the same package, the **DRV8837** driver is selected to ensure the 2 PWM wiring design of the PCB (The DRV8838 can also be used by changing the control software).

2.2.2 Communications and sensing modules

One of the primary elements that the communication and sensing module must have, is the capability to transfer data with the master host. This allows to reprogram the robot for study purposes or send commands as part of a swarm behavioural evaluation. Another element to be included is a positional communicator or identifier. Even though all agents will be made equal, a colour identifier would be useful to recognize, manually or by computer vision, different agents in a swarm and develop translation evaluations of individual agents within a swarm. As specified

before, peer-to-peer communication between agents is necessary for behavioural development for swarm robotics, and thus, need to be included. All these communication elements will be working together, and thus, no interference should exist between them for optimal functioning.

2.2.2.1 Programming communication

As an autonomous robot, the communications of the agent must be wireless; and thus, radiofrequency, optical or acoustic signals must be used. Acoustic signals, like ultrasound, are discarded due to its high power consumption and low efficiency. Since the capabilities of the robot are to be expanded in different possibilities, compliance with commercial protocols and communications systems were preference. Common radiofrequency communication devices use Bluetooth, Zigbee or Wi-Fi, however, integrated circuits and antennas for Zigbee and Wi-Fi can be considered large for our minimalistic design. Most common optical communications are infrared-based running on custom protocols, however, nowadays more commercial devices are running infrared communication under IrDA protocols. Table 2.3 show the preselected technologies.

Table 2-4 Preselected upwards communication devices

Technology	Bluetooth	IrDA	Custom Infrared
Device model / Driver / Transducer	CYBLE-022001-00	TFBS4711 + MCP2122	PNA1601+ SFH 4053
Operating Voltage (V)	1.8 - 4.5	2.4 - 5.5	1.8 -5.5
Max. Oper. Curr. (mA)	25	11	2
Max. Trns. Spd. (kbps)	723.1	115.2	115.2
Distance (m)	10	1	3
Size (mm^2)	10 x 10	12 x 6	6 x 2
Noise robustness	High	High	Low
Soldering	Complex	Moderate	Easy
Price (EUR €)	11.22	4.75	1.76

Although the Bluetooth module have greater capabilities for distance, transfer speeds, and compliance with more devices nowadays, and, its energy consumption can be significantly reduced due to Bluetooth 4.0, its higher price and complex soldering makes it an out-of-range option for a low budget manually implemented project, however, it could be considered for further versions. Custom infrared could be a profitable option with its size and price, given that it has the same speed as IrDA, however, its additional software coding and low robustness to noise makes it susceptible to interference. Therefore, the **IrDA technology transceiver** is selected.

2.2.2.2 Positional communication

A colour identifier for position can easily be developed using a common RGB LED with an appropriate led driver for each colour; enabling a programmable full colour-spectrum identifier, Table 2-5 shows the preselected RGB LEDs and Table 2-6 the preselected LED drivers.

Table 2-5 Preselected RGB LEDs

Model	CLY6D	LTSC-C19FD1WT	HSMF-C114
Dominant wavelength for Red / Green / Blue (mm)	619 ~ 624 520 ~ 540 460 ~ 480	605 525 470	626 525 470
Power Dissipation for Red / Green / Blue (mW)	130 119 76	75 80 80	48 78 78
Maximum Forward Current for Red / Green / Blue (mA)	50 35 20	30 20 20	20 20 20
Package	6-SMD	4-SMD	0606
Size (mm)	2.80 x 2.80	2.10 x 1.60	1.60 x 1.50
Price (EUR €)	0.46	0,48	2.18

Due to its low price, power and current homogeneity, the **LTSC-C19FD1WT** is selected. Its size is sufficiently small and its red spectral bandwidth is fairly

separated from the IrDA bandwidth of 880-900 mm, so no interference will be presented.

Table 2-6 Preselected LED drivers

Model	AP5724	XRP7620	TLC59731
Number of channels	1	4	3
Resolution (bits)	--	6	8
Voltage Supply (V)	2.7 - 5.5	2.7 - 5-5	3.0 - 5.5
Maximum Forward Current (mA)	750	31.5	50
Communication	PWM	I^2C	Serial
Package	SOT-26	8-DFN	8-SOIC
Price (EUR €)	0.38	1.77	0.81

Due to its I^2C interface, package sizing, forward current, and sufficient number of channels, the **XRP7620** driver is selected.

2.2.2.3 Peer-to-peer communication and sensing

Most insects have antennae located on their heads. These are used primarily as a sense organ, based on olfactory and tactile receptors. They allow the insects to sense several signals it their environments. They are also used to sense pheromone trails left by one of its peers that wants to be followed, this is called *recruitment* [2, p. 26]. Therefore, a back-to-end IR communication system is proposed. Each agent will have an IR transmitter on their back; so other agents can sense it, just as "leaving a trail". Location or other custom messages can be broadcasted using modulation. Two IR receivers will be allocated on the front as antennae, one on each side, enabling it to sense and triangulate its peer's trail using stereoscopy or sense obstacles with IR transmitters as well. Table 2.6 shows preselected IR receivers.

Table 2-7 Preselected IR receivers.

Receiver Model	PT12-21C	PNA1601M	SFH3204
Maximum Collector-Emitter Voltage (V)	30	20	15
Maximum Collector Current (mA)	50	20	15
Half-power angle (°)	--	35	60
Peak Sensitivity wavelength (nm)	940	850	920
Typ. Rise-time/Fall-time (µs)	15	4	7
Package type	SMD	Through-hole	Through-hole
Price (EUR €)	0.29	0.73	0.88

Even though **PNA1601M** was not selected for the programming communication in 2.2.2.1; it is selected for this task due to its small rise time, fall time, and restricted angle. Its package has a fixed positioning in assembly, reducing a possible induced error in triangulation calculations. Also, its wavelength bandwidth do not interfere with the IrDA spectrum, preventing interference. Its previously presented transmitter is also selected for this communication and shown in Table 2-8.

Table 2-8 IR transmitter

Receiver Model	SFH 4053
Forward voltage (V)	1.6
Forward current (mA)	70
Half-power angle (°)	70
Peak wavelength (nm)	850
Price (EUR €)	0.88

2.2.3 Control and data processing module

In able to develop a control and data processing module for the robot agent, a microcontroller must be added to control all previous selected electronic components and be capable of process acquired data. One of the most popular microprocessor

nowadays it the ATMEGA328P, due to its use in Arduino boards [23]. The Atmega328P has sufficient resources and peripherals to control our board, as shown in Table 2-9. It can work from 1.8 to 5.0 V and up to 20MHz, giving a sufficient processing speed for the micro-robot. Therefore, by using this microprocessor, our system can be developed and could expanded over to work with Arduino programming sketch files, as stated in the design considerations on 2.1.

Table 2-9 Microcontroller characteristics and system requirements

Receiver Model	Requirements	Characteristics
Operating Voltage (V)	3.3	1.8-5.0
PWM Channels	2	6
Communication	USART, I2C	USART, I2C, SPI
ADC Channels	2	8
I/O Ports	1	21

2.2.4 Power management module

Since our micro-robot has to be autonomous for the purpose of swarm robotics, it must contain a portable battery and all additional circuitry to distribute its power and enable recharging.

2.2.4.1 Battery

To comply with the small size of the agent, batteries with the necessary operating voltage, are preselected according to its optimal energy/size/weight ratio and price. Table 2-10 shows the preselected batteries.

Table 2-10 Preselected batteries

Model	P -1S5045BC	PRT-00731	GM51215
Type	Li-ion	Li-ion	Li-ion
Voltage (V)	4.1	3.7	3.7
Capacity(mAh)	40	100	50
Size (mm)	12 x 16 x 5	12 x 28 x 5.7	12 x 15 x 5
Weight (g)	2	2.65	1.2
Price (EUR €)	4.11	6.34	8.49

Although GM51215 has a small size and weight; its price is too elevated for its capacity. It would be preferable to increase the running time of the battery, and thus; **PTR-00731** is selected.

2.2.4.2 Battery charger

Table 2-11 shows the preselected Lithium-ion battery chargers for the agent. Small size, price, and charge current will be considered.

Table 2-11 Preselected Battery Chargers

Model	AAT3681A	MCP73811T-420I	STC4054
Voltage Supply (V)	4 – 7.5	3.75 - 6	1.5 – 5.5
Charge Voltage (V)	4.2	4.2	4.2
Max. Charge curr. (mA)	500	500	800
Package (g)	8SC70JW	SOT23-5	SOT23-5
Price (EUR €)	0.45	0.48	1.4

Since all preselected devices comply with the charge voltage and current, The **MCP73811T-420I** is selected due to its low price and small package.

2.2.4.3 Voltage regulator.

In order to reduce power consumption and stabilize supply voltages for the integrated circuits, low-drop voltage regulators are used. 1.8V is defined for control signals (microprocessor), and 2.5V is used for IrDA communications. LED drivers and motors will keep working with the battery voltage due to their voltage ratings. Integrated circuits **LP2992AIM5-1.8** and **LP2992AIM5-2.5** are selected, since they have been used in previous works. Their characteristics are displayed in Table 2-12.

Table 2-12 Selected voltage regulators

Model	LP2992AIM5-1.8	LP2992AIM5-2.5
Operating Voltage (V)	2.2-16	2.2-16
Output Voltage(V)	1.8	2.5
Max. Out. Current (mA)	250	250
Output Voltage Accuracy (%)	1	1

2.2.5 Additional Parts.

Additional parts and components were selected and used for the development of the electronic board, including resistors, capacitors, power and expansion connectors, and a power switch. These components, were selected to enhance low power consumption and ensure the functionality of the robot. Additional information can be found on the schematic circuits and part list.

2.2.6 Developed hardware designs

2.2.6.1 Schematic diagram

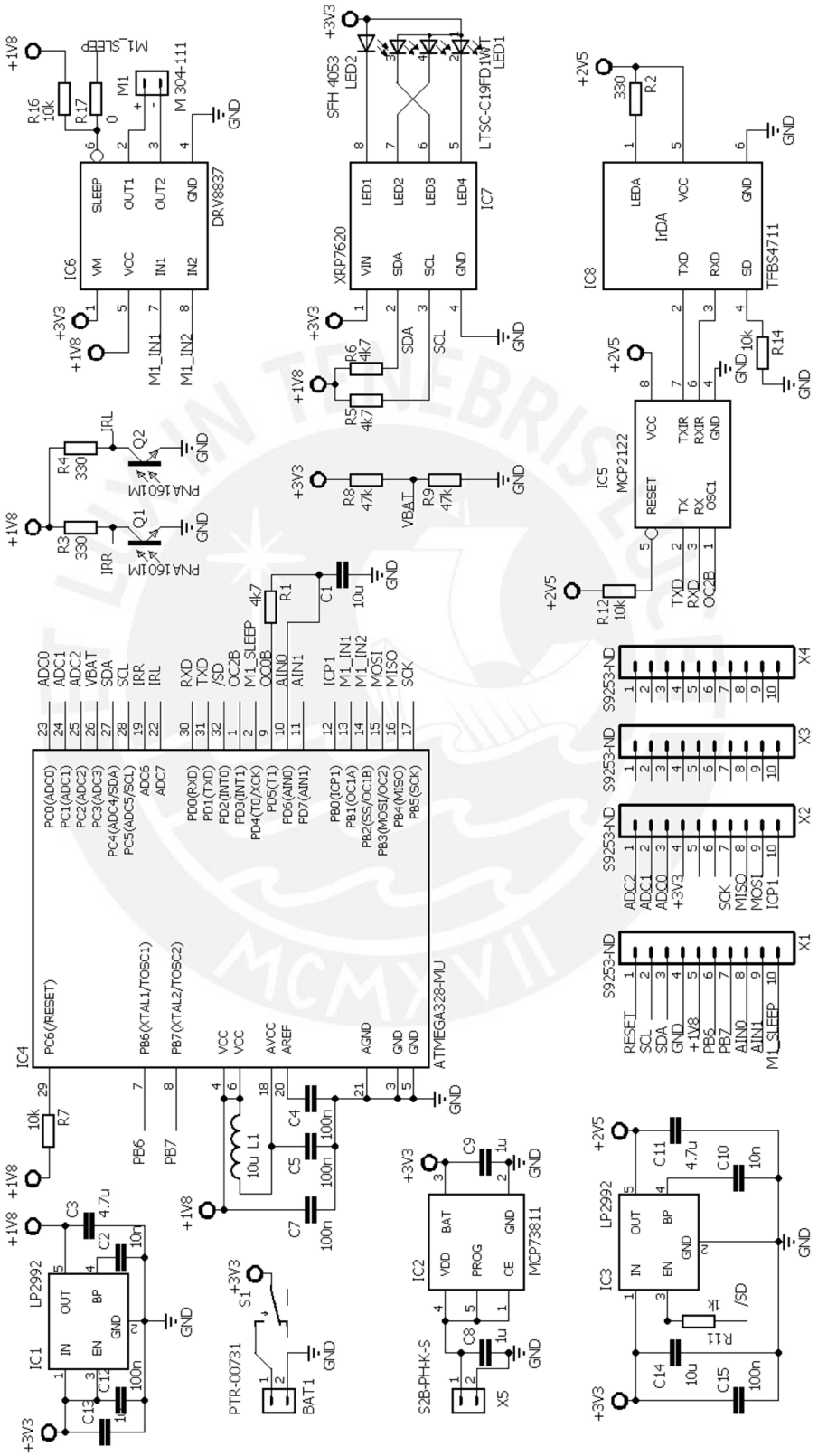

Figure 2.1 Schematic diagram: electronic module of the micro-robot agent.

2.2.6.2 Printed circuit board

Figure 2.2 shows the printed circuit board designs of the micro-robot agent. It is developed over two copper layers, metallized vias, and routes with a minimum 0.254 mm width. The ½ oz. copper films of the layers are located over a FR-4 insulating fiberglass of 1 mm width. Minimum drills diameters are set to 0.3 mm and vias outer ring to 0.5 mm. The board dimensions are 69 x 15 x 1 mm. From left to right of the figure are located both IR sensors and the DC motor. Following is the motor driver, the microprocessor, and the expansion connectors. Then, the IrDA ICs, voltage regulators, battery connector and power switch are located. Finally, the battery charger IC and connector, the LEDs (RGB and IR) and its driver are located.

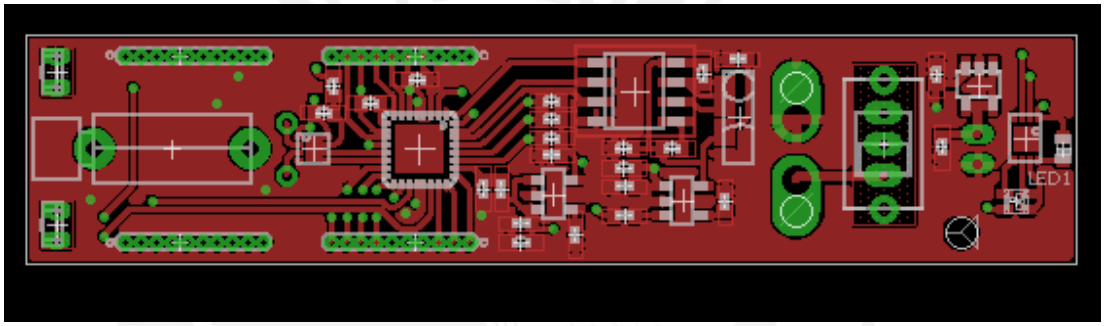

(a) Top layer, top components and vias.

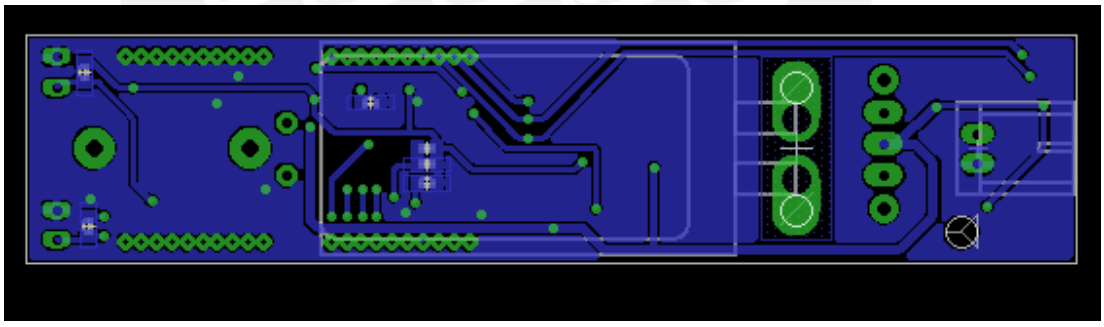

(b) Bottom layer, top components and vias.

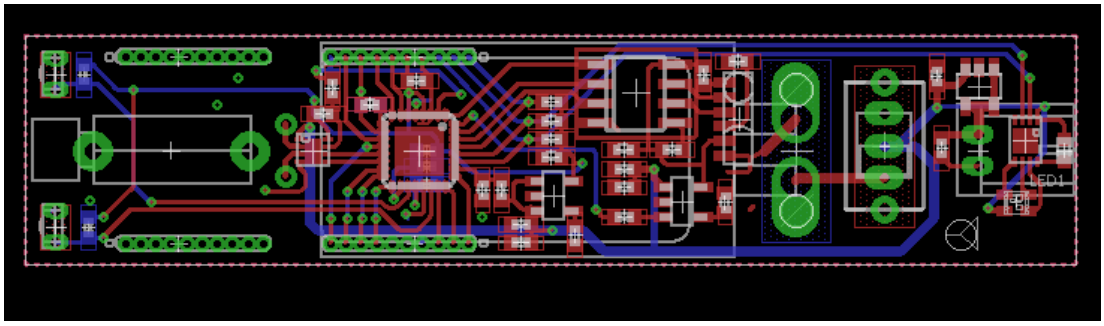

(c) All layers, componets and vias.

Figure 2.2 Designed circuit board: Electronic module of the micro-robot agent.

2.2.6.3 Complete part list

Table 2-13 Bill of Materials of swarm agent

Qty	Value	Device	Package	Parts
1		2_STATES	SWITCH_NO_NC_1	S1
1	0	R-EU_R0402	R0402	R17
5	100n	C-EUC0402	C0402	C4, C5, C7, C12, C15
4	10k	R-EU_R0402	R0402	R7, R12, R14, R16
2	10n	C-EUC0402	C0402	C2, C10
2	10u	C-EUC0402	C0402	C1, C14
1	10u	L-USL0402	L0402	L1
1	1k	R-EU_R0402	R0402	R11
3	1u	C-EUC0402	C0402	C8, C9, C13
3	330	R-EU_R0402	R0402	R2, R3, R4
2	4.7u	C-EUC0402	C0402	C3, C11
2	47k	R-EU_R0402	R0402	R8, R9
3	4k7	R-EU_R0402	R0402	R1, R5, R6
1	ATMEGA328-MU	ATMEGA328-MU	MLF32	IC4
1	DRV8837	DRV8837	DSG8	IC7
1	HSMF-C114	HSMF-C114	LED0606	LED1
2	LP2992	LP2992	SOT23-5	IC2, IC3
1	M 304-111	MOTOR304-111	304-111	M1
1	MCP2122	MCP2122	SO-08	IC5
1	MCP73811	MCP73811	SOT23-5L	IC1
2	PNA1601M	PNA1601M	PNA1601M	Q1, Q2
1	PTR-00731	PTR-00731	PTR-00731	BAT1
1	S2B-PH-K-S	S2B-PH-K-S	PH-SIDE-2POS-2MM	X5
4	S9253-ND	MA10-1-1MM	1MM-8	X1, X2, X3, X4
1	SFH 4053	LEDCHIP-LED0603	CHIP-LED0603	LED2
1	TFBS4711	TFBS4711	TFBS	IC6
1	XRP7620	XRP7620	DFN8	IC8

2.2.7 Control and communication algorithms

As mentioned in Section 2.2.3, the ATMEGA328PA microprocessor will handle all control and communication processes, and thus, the developed algorithms will be based on its internal peripherals and architecture. For the locomotion study, all commands will be received by the programming communications via IrDA technologies, and, although the hardware capabilities will be enabled, no interaction with other agents will be developed yet. A main algorithm is defined in Figure 2.3. All specific functions and procedures are detailed on its corresponding subroutines.

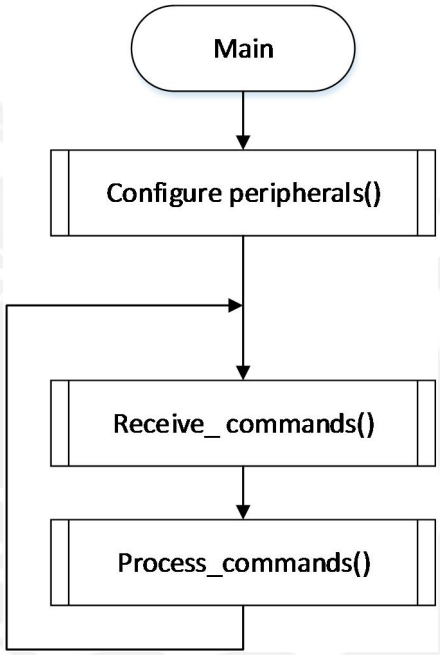

Figure 2.3 Main algorithm of the microprocessor.

2.2.7.1 Motor control subroutines

The next subroutines are developed based on the truth table of the control signals for the motor driver DRV8837 and the configuration of the 16-bit Timer/Counter 1 of the microprocessor Atmega328. The configuration subroutine sets the timer to a Phase correct PWM mode (mode 1) and a frequency of 1.96 kHz (prescaler =1). The control subroutine manages the rotation frequency and direction of the vibro-motor by varying the output channel and duty cycle of the PWM signal. Its inputs are SPEED, a percentage value (%) from 0 to 100; and DIRECTION, a custom variable with pre-set values for each type of movements: CLW (Clockwise), CCW (Counter clockwise), STP (Stop), and FRN (Free Run).

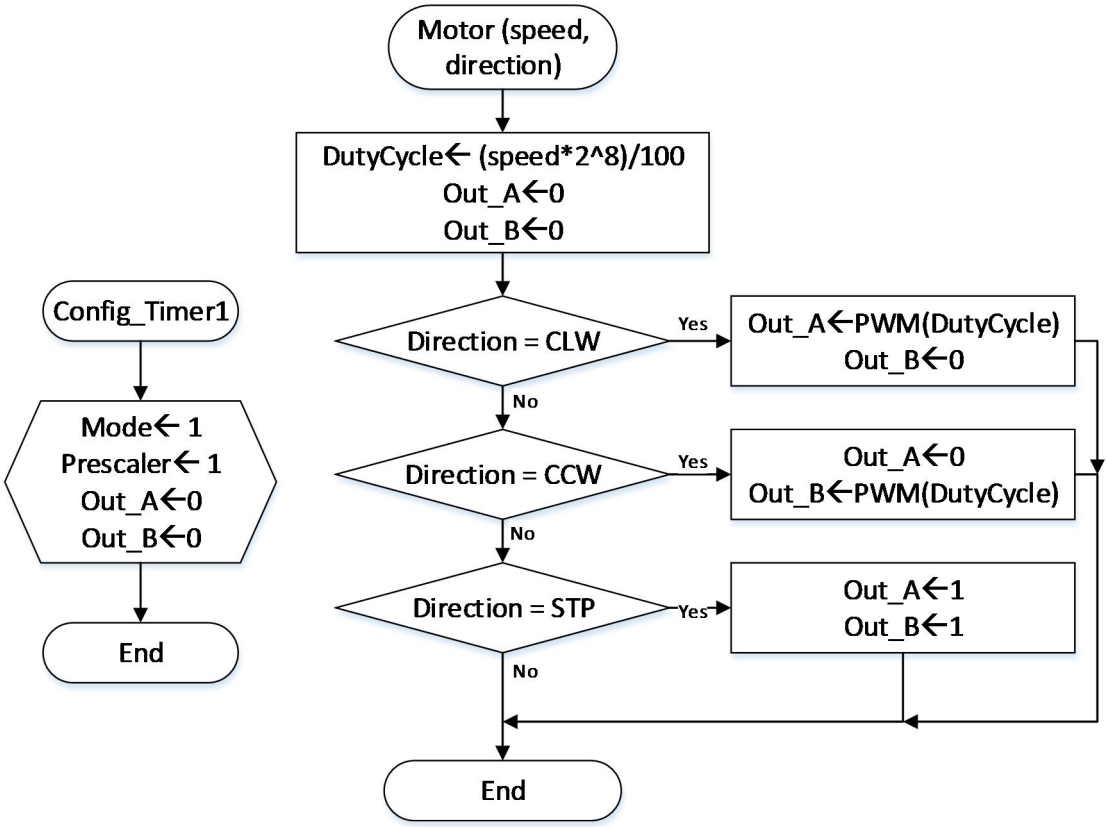

Figure 2.4 Timer/Counter1 configuration and motor control subroutines.

2.2.7.2 IrDA communications subroutines

The IrDA communications are based on the USART and Timer/Counter2 peripherals of the Atmega328PA. The USART controls the data flow and the Timer/Counter2 generates an external 16x clock for the MC2122. An asynchronous, 8 bit, no parity, 1 stop bit and 2400 bps configuration is selected for the USART, and a CTC mode (mode 2) and clock frequency of 38.4 kHz (prescaler =2, OCR2B=12) is generated using Timer2.

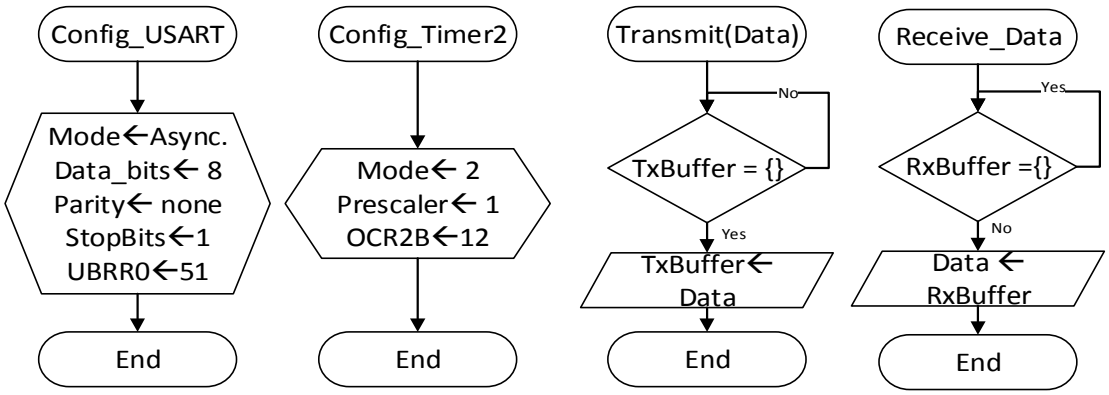

Figure 2.5 Configuration, transmit and receive subroutines of USART and Timer2

To enable a robust communication between the agent and the programming and control interface, a basic protocol was developed to transfer and reproduce locomotion commands. This new protocols allows to send numerous commands controlling the speed, direction, length, delays, repetition, and LEDs status. All sent commands will be reproduced sequentially. The Validate_Header subroutine evaluates if the received bytes correspond to a communication with the programming interface itself. The Add_Move subroutine receive the corresponding bytes of a command and its movements. The Receive_Commands subroutine is one of the main function. It invokes the previous subroutines to receive all sent commands. For a detailed description of the protocol please refer to section 0.

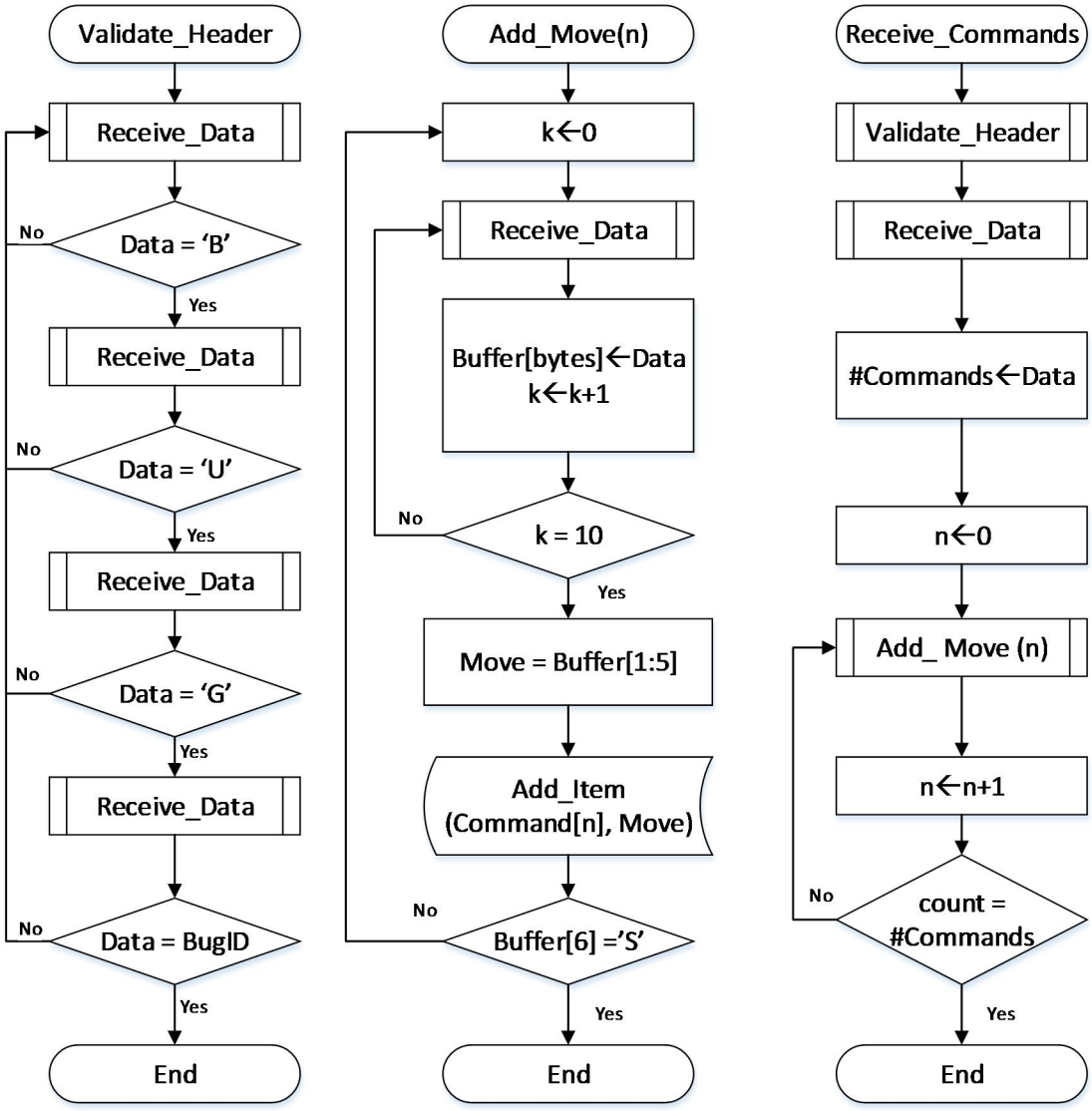

Figure 2.6 Subroutines for receiving movement commands.

2.2.7.3 Peer-to-peer and Positional communication subroutines

To develop the control algorithms for peer-to-peer and positional communications, two peripherals are used: the 2-wire serial interface (TWI) and the Analog-to-Digital Converter (ADC) modules. Using the TWI peripheral, an I^2C-compliant communication is developed to control the XRP7620 using the specifications defined in its datasheet. A 31 kHz frequency is selected (prescaler =1, TWBR =1). One channel controls the peer-to-peer transmit IR LED and the other three control the positional RGB LED. The ADC is configured to its maximum operation frequency at 38.5 kSPS with 8 bits of resolution, and uses channels 6 and 7 for the right and left IR sensors, respectively. These subroutines are shown in Figure 2.7.

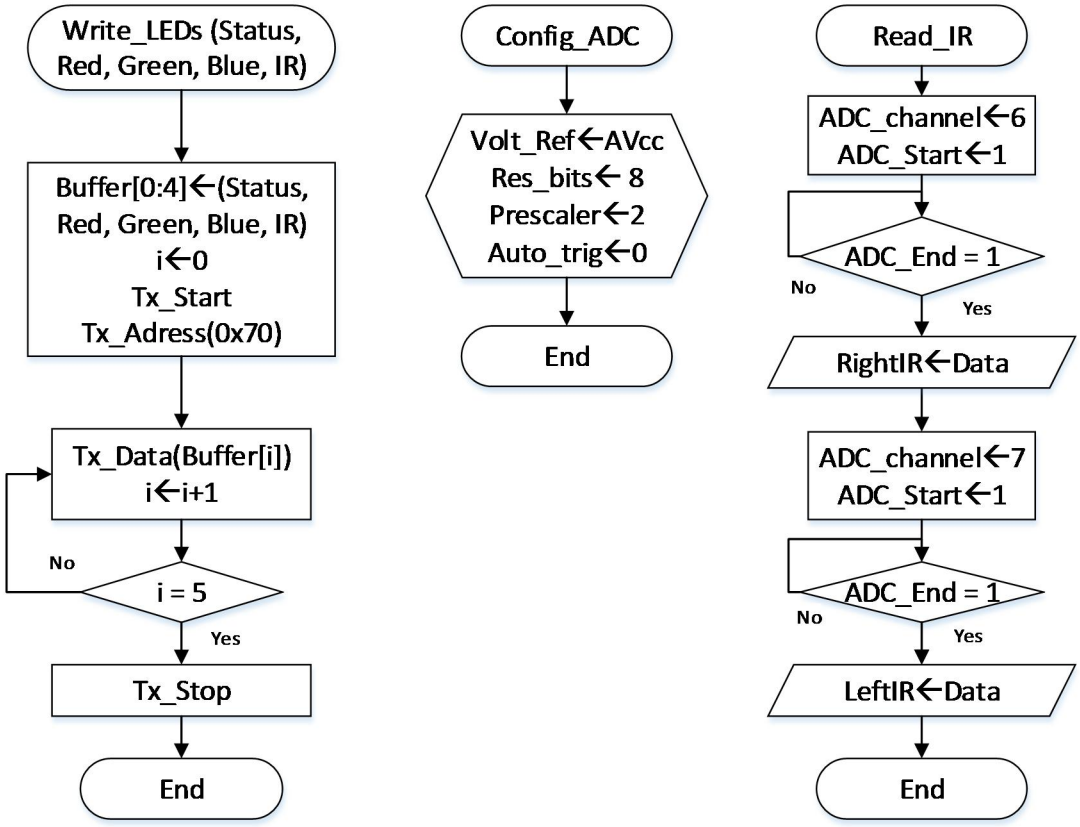

Figure 2.7 TWI and ADC subroutines for peer-to-peer and positional communications

2.2.7.4 Configure peripherals and process commands subroutines

The Configure_peripherals and the Process_commands subroutines are two of the core subroutines shown in Figure 2.3. The first groups all configuration subroutines. The second, processes the received commands to execute the necessary motor and

LED controls in order to develop all associated movements. These subroutines are shown in Figure 2.8.

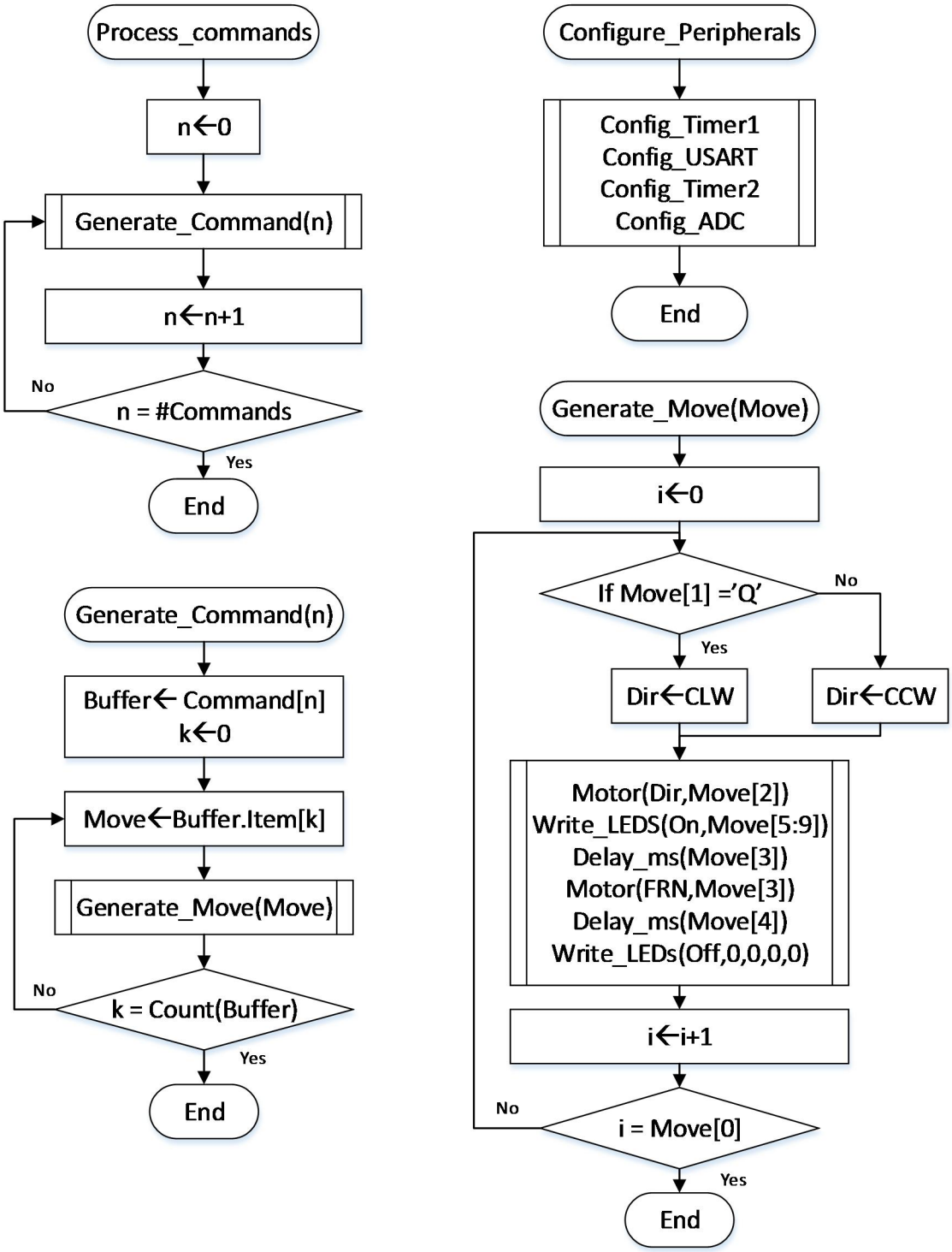

Figure 2.8 Configure peripherals and Process commands subroutines

2.3 Mechanic subsystem

In this section, the selected materials, mechanical design of the locomotion module, and a mathematical model to analyse the robot behaviour are presented.

2.3.1 Locomotion module

The chassis was developed based on the mechanical design and materials of the spy vibro robot of Lysenko et al. [21]. The main chassis is made of a black thermo retractile tube moulded by heat to fit the assembled electronic board. The front and back sides remain free and uncovered to allow light emissions of the IR and RGB LEDs and infrared sensors. An incision is made on the top to allow light emissions of the IrDA transceiver. The bristles, made from a flexible foam plastic, are attached to the chassis bottom part in a two-row configuration. The architecture of the chassis enables the possibility to develop several simple bodies with different bristles and exchange them at any time without the use of additional tools. Two markers are added on the centre and frontal sides of the robot for motion tracking aid.

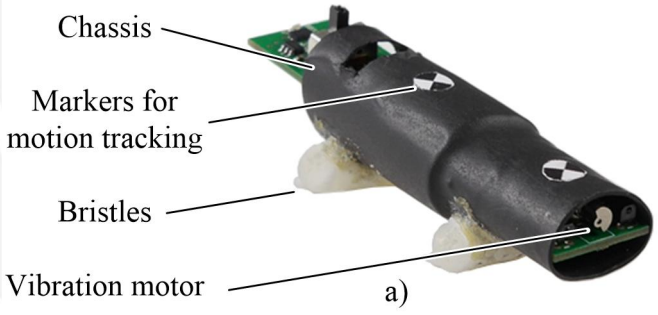

a) Mechanical chassis

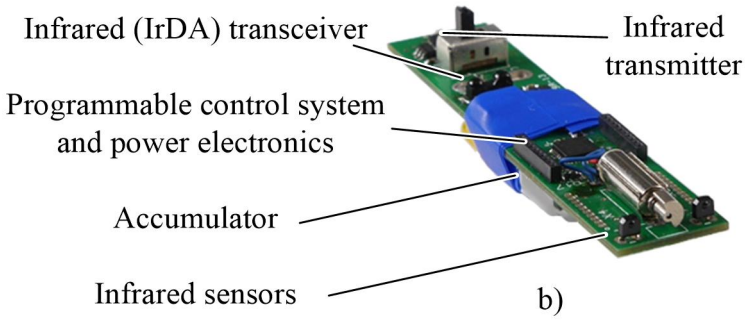

b) Internal Electronic system

Figure 2.9 Design prototype of the bristle-based swarm agent.

2.3.2 Mechanical model

For swarm simulations the underlying mechanical model of an agent should be as simple as possible, but comprises the dominant locomotion mechanisms. The analyses of the motion behaviour of bristlebots show that locomotion is determined by periodic actuation forces and non-symmetric friction forces. In Figure 2.10 the proposed mass point model is presented.

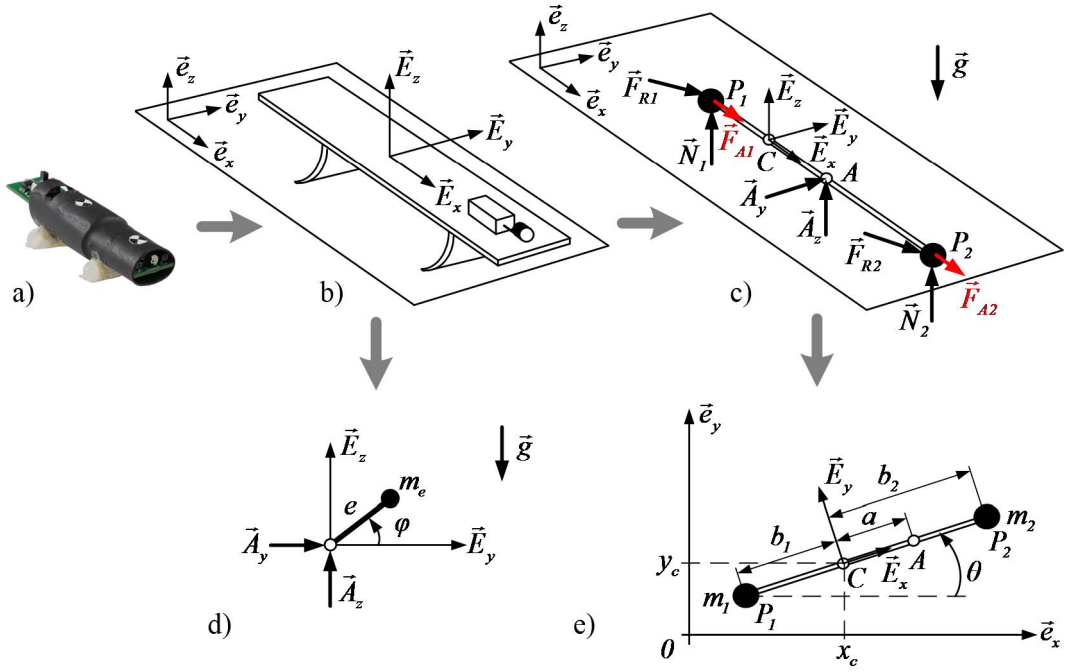

a) Robot prototype; b) Schematic robot; c) Robot model with forces; d) Motor model; e) Geometry and coordinates.

Figure 2.10 Modeling of the robot

The system is composed by two mass points P_1 and P_2 which carry the masses m_1 and m_2, respectively. They are connected by a massless bar of length $\overline{CP_1} + \overline{CP_2} = b_1 + b_2$. Two Cartesian coordinate systems are introduced: a fixed reference frame with the unit vectors $(\vec{e}_x, \vec{e}_y, \vec{e}_z)$, and a body-attached frame with $(\vec{E}_x, \vec{E}_y, \vec{E}_z)$, which is situated in the center of mass $C(x_c, y_c, z_c)$. The motion of the system is limited to the plane $(\vec{e}_x, \vec{e}_y)$, therefore $\vec{e}_z = \vec{E}_z$, and the number of degrees of freedom is set to three. With the angle $\theta = \angle(\vec{e}_x, \vec{E}_x)$, the transformation equation follows

$$\begin{aligned} \vec{e}_x &= \cos\theta\,\vec{E}_x - \sin\theta\,\vec{E}_y, \quad \vec{E}_x = \cos\theta\,\vec{e}_x + \sin\theta\,\vec{e}_y \\ \vec{e}_y &= \sin\theta\,\vec{E}_x + \cos\theta\,\vec{E}_y, \quad \vec{E}_y = -\sin\theta\,\vec{e}_x + \sin\theta\,\vec{e}_y \end{aligned} \tag{1}$$

The vibration motor generates the forces $\vec{A}_y$ and $\vec{A}_z$ at the point A. They are determined by the motion of the eccentric mass m_e on a circular orbit with radius e and angular velocity $\dot{\varphi} = \Omega$ in the plane $\left(\vec{E}_y, \vec{E}_z\right)$, giving :

$$\begin{aligned} \vec{A}_y &= -m_e e\Omega^2 \cos\Omega t\,\vec{E}_y, \\ \vec{A}_z &= -\left(m_e g - m_e e\Omega^2 \sin\Omega t\right)\vec{E}_z. \end{aligned} \tag{2}$$

At the points P_1 and P_2, normal forces $\vec{N}_1, \vec{N}_2$; Coulomb dry friction forces $\vec{F}_{R1}, \vec{F}_{R2}$; and actuation forces $\vec{F}_{A1}, \vec{F}_{A2}$; are applied. The actuation forces are modelling the periodic forward forces produced by the elastic bristles due to the excitation of the motor:

$$\vec{F}_{A1} = F_{A1} \sin\Omega t\,\vec{E}_x, \qquad \vec{F}_{A2} = F_{A2} \sin\Omega t\,\vec{E}_x. \tag{3}$$

As the actuation forces of bristles are developed by the frictional contact between the robot and ground, the magnitudes F_{A1} and F_{A2} may not exceed the friction forces in backward direction. The normal forces $\vec{N}_1 = N_1\vec{E}_z$ and $\vec{N}_2 = N_2\vec{E}_z$ can be calculated using the equilibrium of forces in the $\vec{e}_z$-direction and the equilibrium of moments about $\vec{E}_y$:

$$\begin{aligned} 0 &= N_1 + N_2 + A_z - \left(m_1 + m_2\right) g, \\ 0 &= -b_1 N_1 + b_2 N_2 + a A_z. \end{aligned} \tag{4}$$

With $\overline{CA} = a$, it follows:

$$\begin{aligned} N_1 &= \frac{b_2}{b_1 + b_2}\left(m_1 + m_2\right) g + \frac{b_2 - a}{b_1 + b_2}\left(m_e g + m_e e\Omega^2 \sin\Omega t\right), \\ N_2 &= \frac{b_1}{b_1 + b_2}\left(m_1 + m_2\right) g + \frac{b_1 + a}{b_1 + b_2}\left(m_e g + m_e e\Omega^2 \sin\Omega t\right). \end{aligned} \tag{5}$$

In order to fulfill the condition of constant contact, $N_1 \geq 0$ and $N_2 \geq 0$ is needed. To obtain the friction forces,

$$\vec{F}_{R1} = -\mu |N_1| \frac{\dot{\vec{r}}_1}{|\dot{\vec{r}}_1|}, \qquad \vec{F}_{R2} = -\mu |N_2| \frac{\dot{\vec{r}}_2}{|\dot{\vec{r}}_2|} \tag{6}$$

and the velocities of P_1 and P_2 are determined:

$$\begin{aligned} \dot{\vec{r}}_1 &= \dot{x}_1 \vec{e}_x + \dot{y}_1 \vec{e}_y = \left(\dot{x}_c + b_1 \dot{\theta} \sin\theta\right)\vec{e}_x + \left(\dot{y}_c - b_1 \dot{\theta} \cos\theta\right)\vec{e}_y, \\ \dot{\vec{r}}_2 &= \dot{x}_2 \vec{e}_x + \dot{y}_2 \vec{e}_y = \left(\dot{x}_c - b_2 \dot{\theta} \sin\theta\right)\vec{e}_x + \left(\dot{y}_c + b_2 \dot{\theta} \cos\theta\right)\vec{e}_y. \end{aligned} \tag{7}$$

The principle of linear momentum $M\ddot{\vec{r}} = \sum \vec{F}$ can be written in two scalar equations on the fixed reference frame $\left(\vec{e}_x, \vec{e}_y, \vec{e}_z\right)$:

$$M\,\ddot{x}_c = -\mu |N_1| \frac{\dot{x}_1}{|\dot{\vec{r}}_1|} - \mu |N_2| \frac{\dot{x}_2}{|\dot{\vec{r}}_2|} + m_e e \Omega^2 \cos\Omega t \sin\theta + \left(F_{A1} + F_{A2}\right) \sin\Omega t \cos\theta, \tag{8}$$

$$M\,\ddot{y}_c = -\mu |N_1| \frac{\dot{y}_1}{|\dot{\vec{r}}_1|} - \mu |N_2| \frac{\dot{y}_2}{|\dot{\vec{r}}_2|} - m_e e \Omega^2 \cos\Omega t \cos\theta + \left(F_{A1} + F_{A2}\right) \sin\Omega t \sin\theta, \tag{9}$$

where $M = m_1 + m_2 + m_e$ and $\ddot{\vec{r}} = \ddot{x}_c \vec{e}_x + \ddot{y}_c \vec{e}_y$. The principle of angular momentum $\dot{\vec{D}}_C = \sum \vec{M}_C$ is applied in the center of mass C with $J = m_1 b_1^2 + m_2 b_2^2 + m_e a^2$ and $\dot{\vec{D}}_C = J\ddot{\theta}\vec{E}_z$:

$$J\ddot{\theta} = -a\, m_e e \Omega^2 \cos\Omega t - b_1 \mu |N_1| \frac{1}{|\dot{\vec{r}}_1|}\left(\dot{x}_1 \sin\theta - \dot{y}_1 \cos\theta\right) - b_2 \mu |N_2| \frac{1}{|\dot{\vec{r}}_2|}\left(\dot{x}_2 \sin\theta - \dot{y}_2 \cos\theta\right). \tag{10}$$

2.3.3 Simulations

Simulations were conducted in MATLAB/Simulink to analyze the presented model. The values of the parameters, which refer to the prototype presented in Figure 2.10, are given in Table 2-14. It should be mentioned that the parameter range is limited by the condition of constant contact: $N_1 \geq 0$ and $N_2 \geq 0$ discussed previously. Some results of the simulations are presented in Figure 2.11. It shows trajectories of the points P_1, P_2 and C for different values of parameters. It may be seen that the robot model moves on a curved orbit. The radius of the trajectory and the velocity depend on the rotational speed of the motor Ω . The turning direction of

the model can be controlled by the sign of Ω . The position of the mass m_e relative to the center of mass C of the overall system is labeled with a. The influence of a to the orbit due to the produced torque is also presented in Figure 2.11. It is obvious that the increasing overall mass $M = m_1 + m_2 + m_e$ reduces the velocity. Moreover, the system moves faster for a small friction coefficient μ.

Table 2-14 Model parameters used in the simulations.

Model geometry		b_1	15 mm		b_2	15 mm	a	33 mm
Mass distribution		m_1	5 g		m_2	5 g	J	2.5 kg mm²
Motor parameters		m_e	0.3 g		e	0.2 mm	Ω	-6000 rpm
Environment		g	9.81 m/s²		μ	0.05	t	0... 10 s
Actuation forces		F_{A1}	0.0624 N		F_{A2}	0.0624 N		

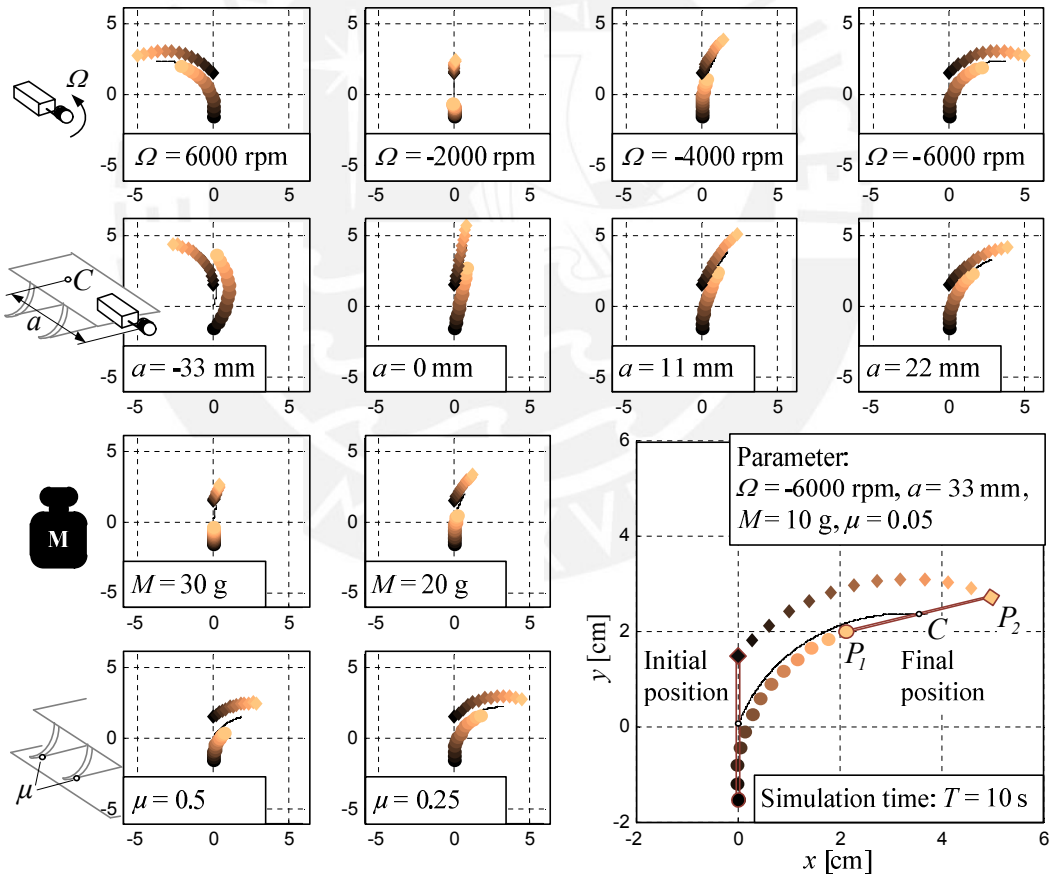

Figure 2.11 Numerical parameter study: trajectories of the points P1, P2 and C for different values of parameters

CHAPTER III

DESIGN OF THE PROGRAMMING AND CONTROL INTERFACE

This chapters exposes the software and hardware electronic designs for the programming and control interface for the swarm robotic system. Its design is based upon the interface section of the preliminary block diagram shown in Figure 1.8.

3.1 Design considerations

Some considerations based on a priori knowledge, the design of the agent, and basic elements are given in order to achieve the proposed objectives of this work. These are presented in Table 3-1

Table 3-1 Design considerations for the programming and control interface

Criteria	Specification	Priority
General		
Reproducibility	Design must be reproducible	High
Price	Low	Low
Main Programming Module		
Platform	PC	High
Environment and Language	Microsoft Visual Studio C#	Medium
Communications	Serial Port	High
Communications protocol	Custom	High
Communications Adapter		
Physical Layer	USB to IrDA	High
Energy	External +5V supply from PC	High
Image Processing Module and Camera		
Image processing mod.	Module capable of processing the Positional RGB LED of the agent	None
Camera	Camera connectivity with processing module	None

Developed by the author.

3.2 Communications protocol

A communication protocol is defined in order to transfer data packages containing commands to a robot agent. These commands generate the necessary control signals for locomotion development and control of the LEDs. The Overall protocol can be seen in Figure 3.1.

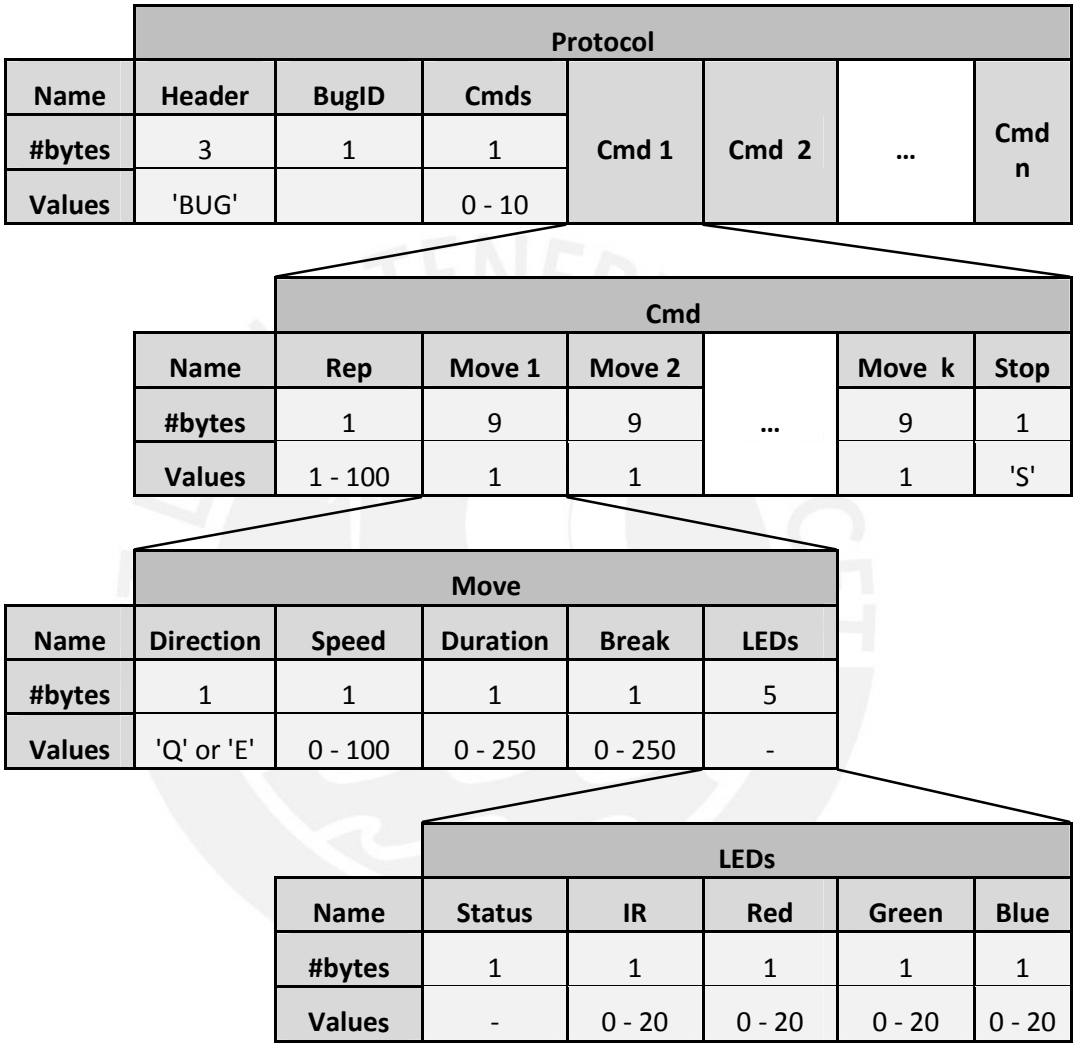

Figure 3.1 Command transmission protocol

The main level protocol contains a *Header, BugID*, *Cmds* and the corresponding commands (cmd). The *Header* is an identifier that starts the data transmit. The *BugID* value is used to select the desired agent. If an agent reads its own ID, it will continue the data transmission, otherwise, it will restart its validation process. The *Cmds* byte indicates the quantity of commands that will be transferred.

Each command has its own length due to the quantity of movements (*move*) included. The *Rep* byte indicates the number of repetitions the package of movements on the command will be repeated in a cycle. A *Stop* byte is used after all the movements to determine the end of the command.

Each movement has a length of 9 bytes. *Direction, Speed* and *Duration* define the direction, and speed of the rotation of the vibro-motor, and the duration of the pulse, respectively. The *Break* byte defines the stand-by delay after the vibro-motor has been stopped. Finally, the sub package *LEDs* control the ON/OFF status and intensity of all four LEDs.

3.3 Control and programming interface

The development of the control and programming interface will require to contain all necessary tools for developing the locomotion studies of the swarm agent, and thus, a simple system is proposed. The system will have a GUI capable of creating commands with a set of easy-to-use fields and buttons; a list to display all stored commands that will be sent, and a programming button to transfer all stored commands by the serial port to the swarm agent.

3.3.1 Graphic User Interface (GUI)

The GUI is divided in 5 parts that help the user to configure the serial port, create new commands; and send them to the specified robot. Figure 3.3 shows the developed graphic user interface and its elements. In section A) a set of controls is developed to select and activate the serial port connected to the IrDA adapter. Section B) enables the selection of the target swarm agent. (In this case, the preselected ID will always be “1”). Section C) enables the creation of a new command, and D) the creation of new movements to the established command. At last, section E) shows the list box with all created commands and a button to initiate the transfer.

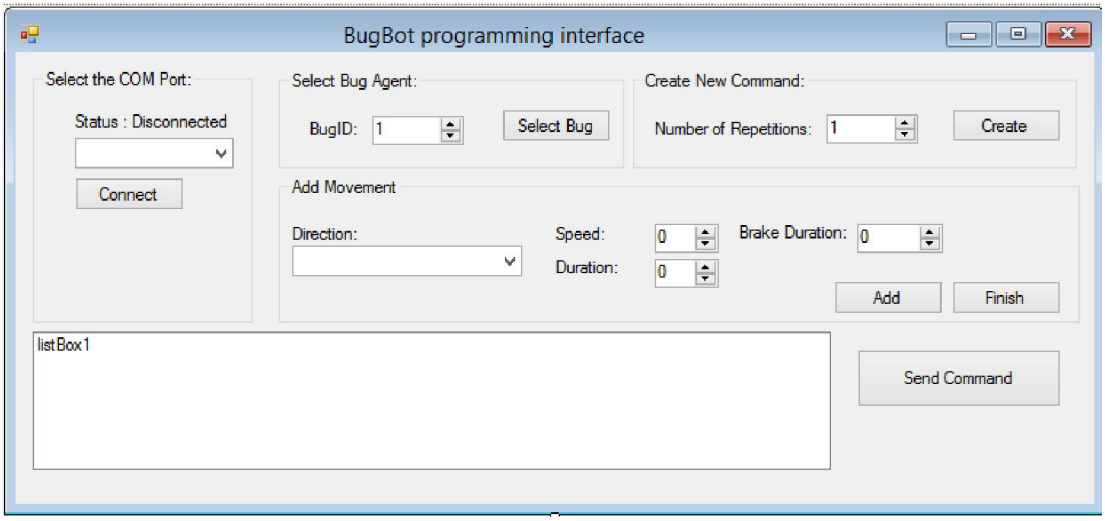

(a) Graphic User Interface

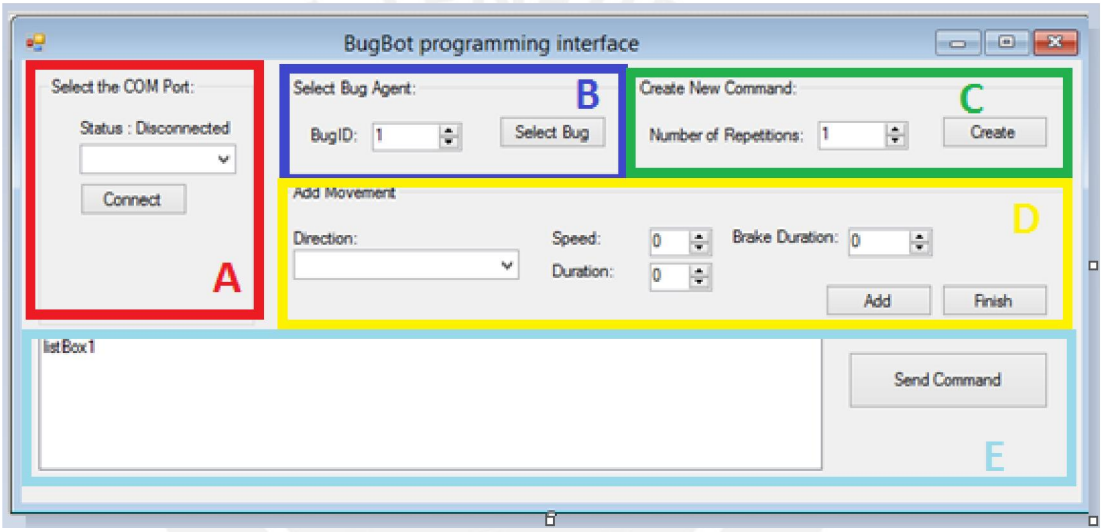

(b) GUI Subsections: A) Serial Port configuration, B) Swarm agent selection, C) New command creation, D) Add movements, and E) Commands list box and transfer button.

Figure 3.2 Graphic User Interface and its subsections.

3.3.2 Control Algorithms

For each existing control on the GUI, a subroutine with the necessary control algorithms have been established to enable the functionality of the programming interface. Figure 3.4 shows the main functioning algorithms of the GUI.

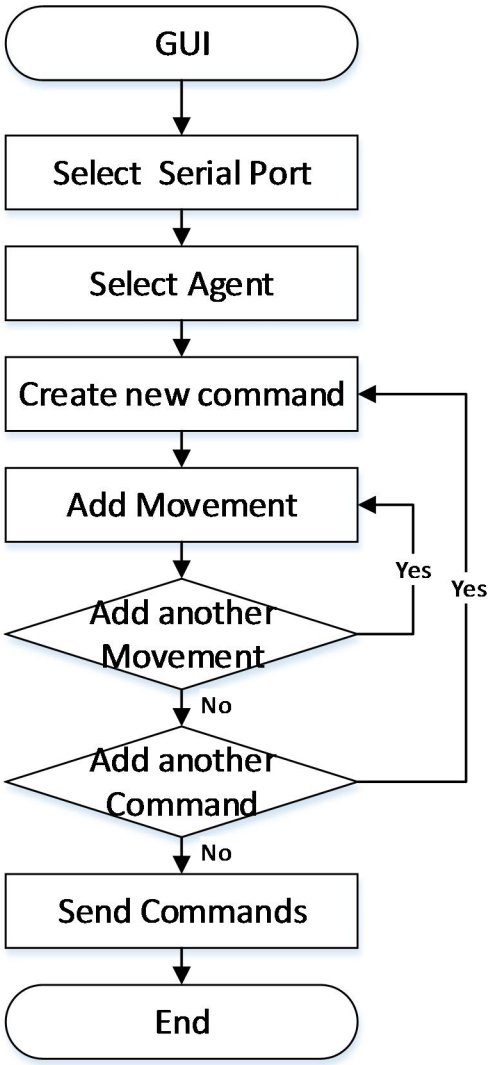

Figure 3.3 Graphic User Interface main functioning algorithm

3.4 Hardware adapter

To develop a hardware adapter to enable communications between the host program and one robot agent, changes in the physical layer of communication must be implemented to go from USB (most common PC port nowadays) to IrDA. Figure 3.4 shows a simple block diagram.

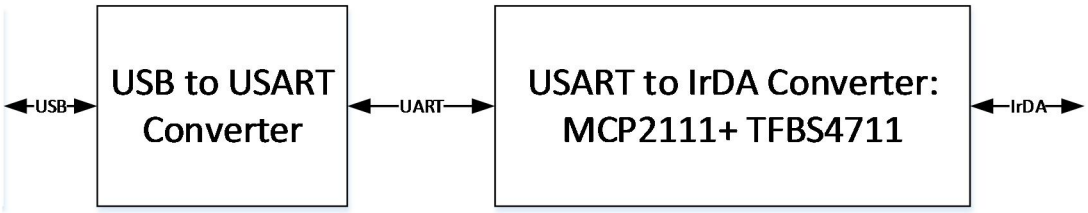

Figure 3.4 Block Diagram of hardware adapter

3.4.1 Component selection

As stated on section 3.1, the UART to IrDA physical layer will be developed with the combination of both integrated circuits MCP2111 and TFBS4711. In able to develop the USB to UART converter, the preselected options are shown in table 3.1

Table 3-2 Preselected USB to UART Converter

Integrated Circuit	FT232	Atmega8U2	USB/UART Module
Operating Voltage (V)	5.0	1.8 – 5.0	3.3 – 5.0
Programmable Firmware	Yes	Yes	No
External clock (MHz)	>2	< 8	No
Variable transfer speed	Yes	Yes	Yes
Price (EUR €)	4.12	3.96	3.04

The FT232 chip from FTDI have been used in the past years for USB to UART bridges in many projects, including the Arduino boards; due to its on-chip USB protocol implementation for a serial ports, however, with the open source LUFA libraries [25] for USB development on Atmel processors, different types of firmware for USB development are available to compile and program on a atmega8u2. Also, the External clock generation for the 16x clock signal for the MCP2111 is required, and, the FT232 chip is only able to produce signals higher than 2MHz, where the Atmega8u2 can produce virtually any frequency up to 8MHz. Therefore, the **Atmega8U2** is selected.

3.4.2 Additional Parts.

Additional parts and components were selected and used for the development of the electronic board, including resistors, capacitors and USB connectors are selected. These components, were selected to to facilitate the use of the USB-IrDA adapter with one robot agent. Additional information can be found on the schematic circuits and part list.

3.4.3 Developed hardware designs

3.4.3.1 Schematic diagram

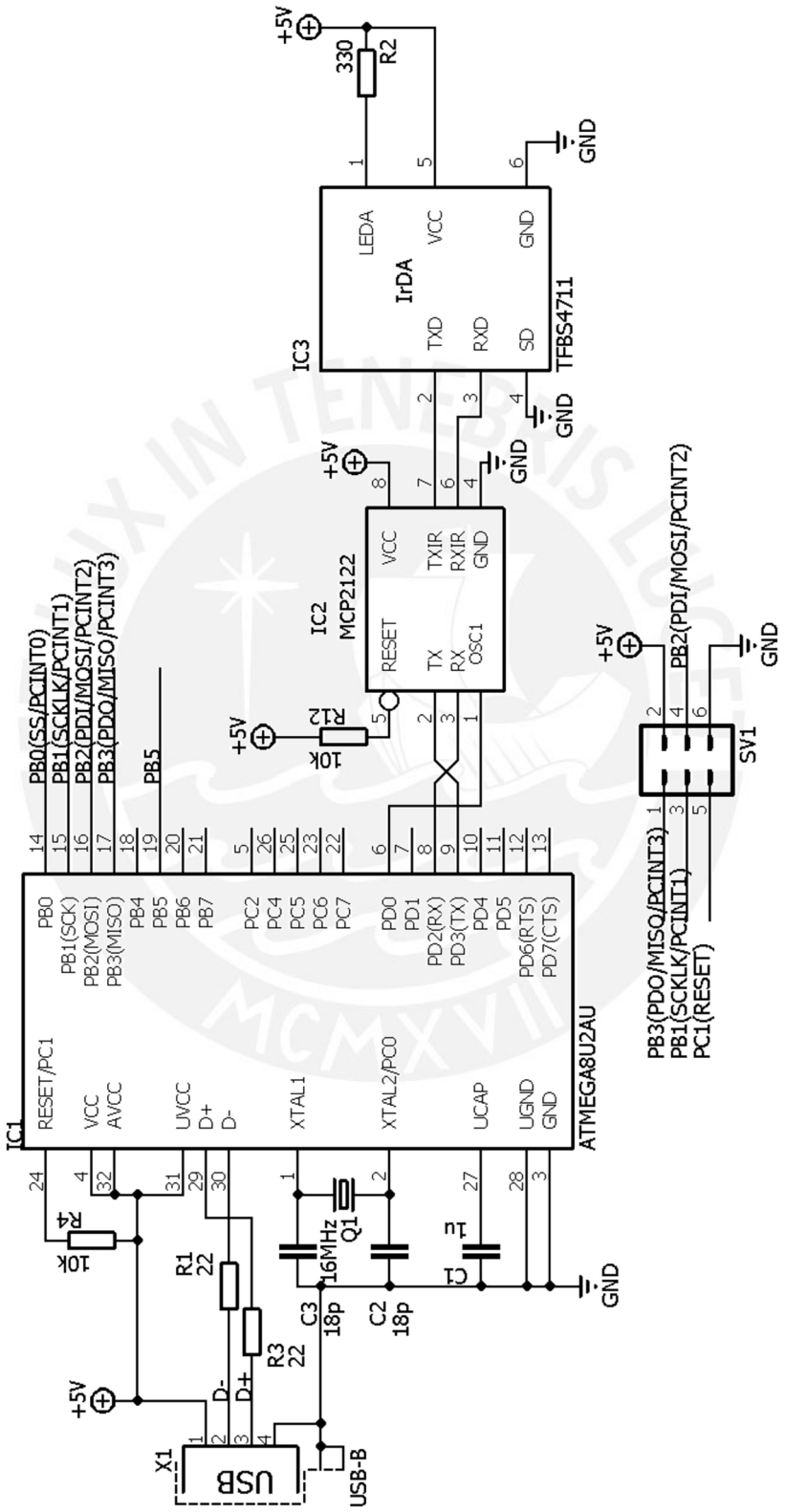

Figure 3.5 Schematic diagram of the USB-IrDA adapter

3.4.3.2 Printed circuit board

Figure 3.6 shows the printed circuit board designs of the USB-IrDA adapter. It is developed over two copper layers and routes with a minimum 0.4 mm width. The 1 oz. copper films of the layers are located over an insulating Bakelite of 1.5 mm width. Minimum drills diameters are set to 1 mm and vias outer ring to 1.5 mm. The board dimensions are 31 x 24 x 1.5 mm. The top layer shows the USB connector, the 16 MHz crystals, and IrDA integrated circuits. The bottom layer shows the microcontroller.

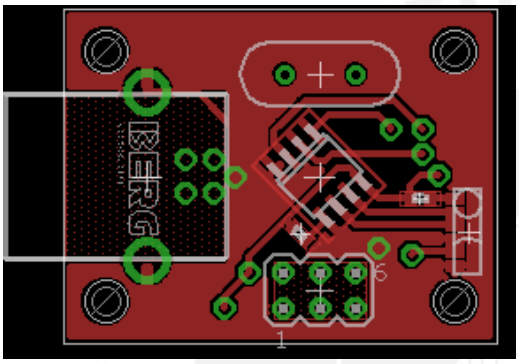

(a) Top layer and components

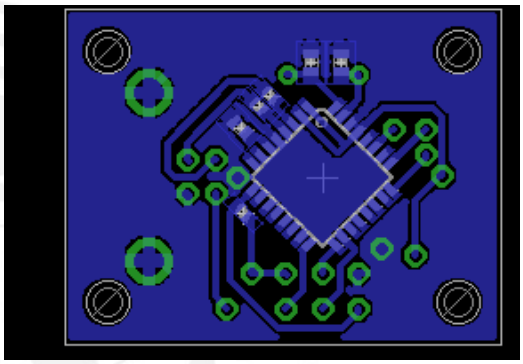

(b) Bottom layer and components

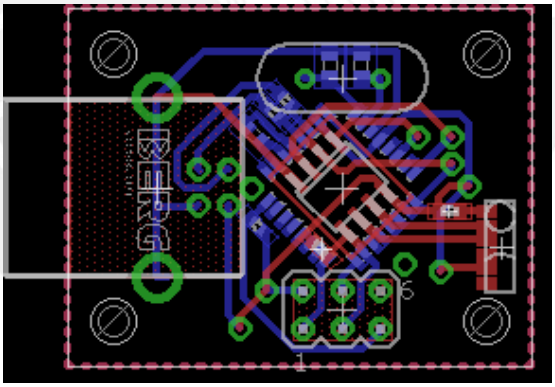

(b) All layers and components

Figure 3.6 Board design of the USB- IrDA adapter

3.4.3.3 Complete part list

Table 3-3 Bill of Materials for the USB-IrDA adapter

Qty	Value	Device	Package	Parts
1		MA03-2	MA03-2	SV1
2	10k	R-EU_R0402	R0402	R4, R12
1	16MHz	CRYSTALHC49US	HC49US	Q1
2	18p	CAP0603-CAP	0603-CAP	C2, C3
1	1u	CAP0603-CAP	0603-CAP	C1
2	22	R-EU_R0402	R0402	R1, R3
1	330	R-EU_R0402	R0402	R2
1	ATMEGA8U2AU	ATMEGA8U2AU	TQFP32-08	IC1
1	MCP2122	MCP2122	SO-08	IC2
1	TFBS4711	TFBS4711	TFBS	IC3
1	USB-B	PN61729-S	PN61729-S	X1

3.4.4 Firmware

As mentioned before, in order to develop the USB to UART Bridge in the Atmega8U2, the LUFA libraries will be used; however, in order to create the 16X clock signal for the MCP2111, small modifications will be required in the firmware to activate the Timer0 to produce the clock signal. Since the LUFA libraries have a high complexity level of understanding to the de USB protocol; no emphasis will be made upon its functioning algorithm.

CHAPTER IV

EXPERIMENTS AND RESULTS

Experimental test are performed to measure and evaluate the displacement capabilities and trajectory generation of the designed robot agent. Using the control and programming interface developed on the previous chapter, different commands were programmed on the agent for each experiment. A kinematic analysis is developed based on the agent model to extract the desired characteristics. Basic experiments show the capability for displacement (movement generation) with both rotation directions and several speeds. Advanced experiments show the capability for trajectory generation using combined movements.

4.1 Kinematic analysis

A kinematic analysis was developed based on an agent model to extract desired velocities and rotation characteristics. Given the diagram displayed in Figure 4.1, the positional vectors of the markers on the agent were evaluated and expressions for the rotation (ω), parallel ($\vec{v}_p$) and transversal ($\vec{v}_t$) velocities of the robot are defined.

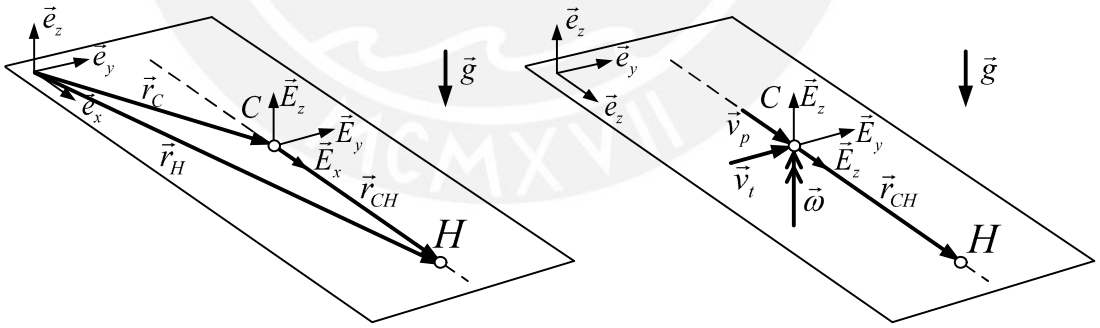

Figure 4.1: Kinematic analysis of markers on the robot agent's. (a) Positional vectors: $\overrightarrow{r_C}$, the position of the centre of mass C; $\overrightarrow{r_H}$, the position of H; and $\overrightarrow{r_{CH}}$ the relative position of H from C. (b) Velocity vectors: $\overrightarrow{v_p}$ is the velocity component of C in the direction of $\overrightarrow{E_x}$; $\overrightarrow{v_t}$, the velocity component of C in the direction of $\overrightarrow{E_y}$; and $\vec{\omega}$, the rotational speed of the agent around C.

The rotation speed $\vec{\omega} = \omega(t)\vec{E}_z$ is given using the angle $\theta = \angle(\vec{e}_x, \vec{E}_x) = \angle\vec{r}_{CH}$, where:

$$\omega(t) = \frac{d\theta}{dt} \tag{11}$$

Perpendicular and transversal speeds of the robot, $\vec{v}_p = v_p(t)\vec{E}_x$ and $\vec{v}_t = v_t(t)\vec{E}_y$ are given using $\vec{v}_C = \dot{\vec{r}}_C = v_x(t)\vec{e}_x + v_y(t)\vec{e}_y$, and the transformation equation (1), where:

$$\begin{aligned} v_p(t) &= \vec{v}_C \cdot \vec{E}_x \\ v_t(t) &= \vec{v}_C \cdot \vec{E}_y \end{aligned} \tag{12}$$

It follows,

$$\begin{aligned} v_p(t) &= \cos\theta\, v_x(t) + \sin\theta\, v_y(t) \\ v_t(t) &= -\sin\theta\, v_x(t) + \cos\theta\, v_y(t) \end{aligned} \tag{13}$$

4.2 Experimental setup

Experimental videos were recorded using a digital camera *(60 FPS, 1080x480 pixels)* installed on a tripod facing the surface platform. Positional data from two markers installed on the agent were acquired from the videos using the ***Tracker*** Computer vision software. To achieve data consistency, each experiment was conducted 10 times. Figure 4.1 shows an acquired frame sample through the Tracker software and its principal elements.

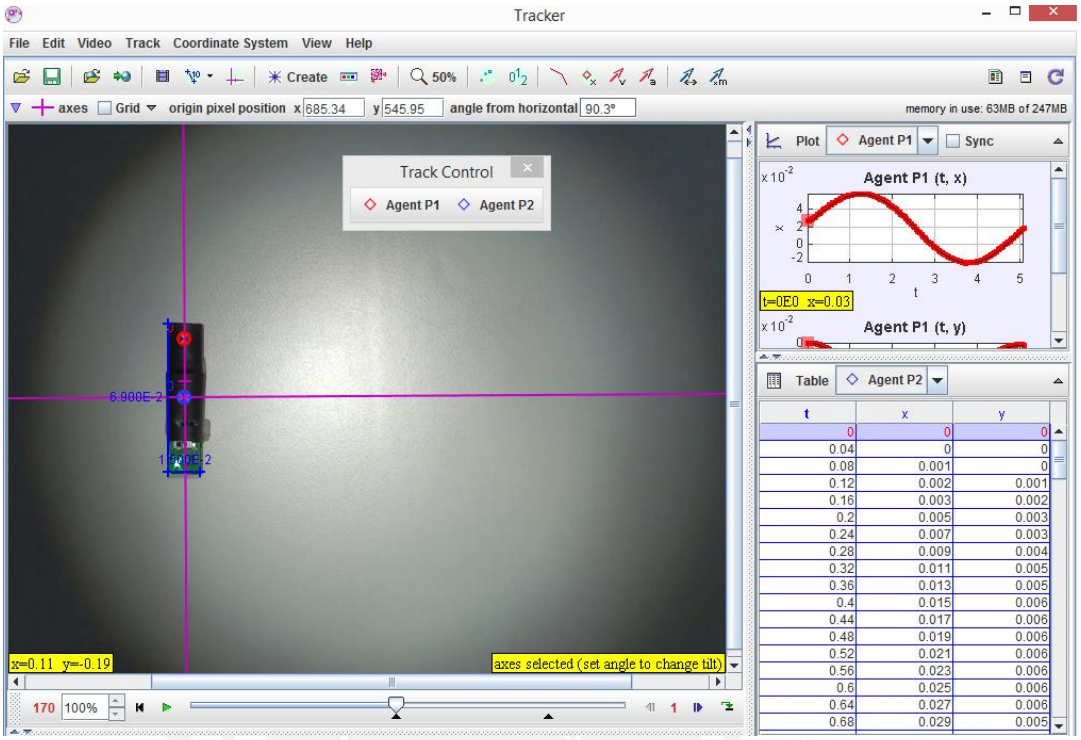

Figure 4.1 Acquired frame using the Tracker software for motion analysis.

4.3 Basic Experiments

Several experiments are conducted to evaluate the displacement and generated velocities for different frequencies in both directions of the vibration motor. Figure 4.2 and Figure 4.3 show the acquired positional data and calculated speeds for a Clockwise (CLW) and Counter Clockwise (CCW) rotations at 170 Hz for 1 second, respectively. All experiments were developed on the same flat surface. A breaking time of 100 μs was set for all movements. Top graphics show the evolution of x and y positions of both markers C and H over time, with remarks on its initial and final positions. The centre graphic shows both markers and its displacement over the *xy*-plane. Bottom graphics show the rotation, parallel and transversal speeds of the robots over time, respectively. The same experiment was developed for both motor rotations at frequencies 170, 190, 210, 230 and 250 H for 1 second. Figure 4.4 shows the average values of the achieved rotation, parallel and transversal speeds.

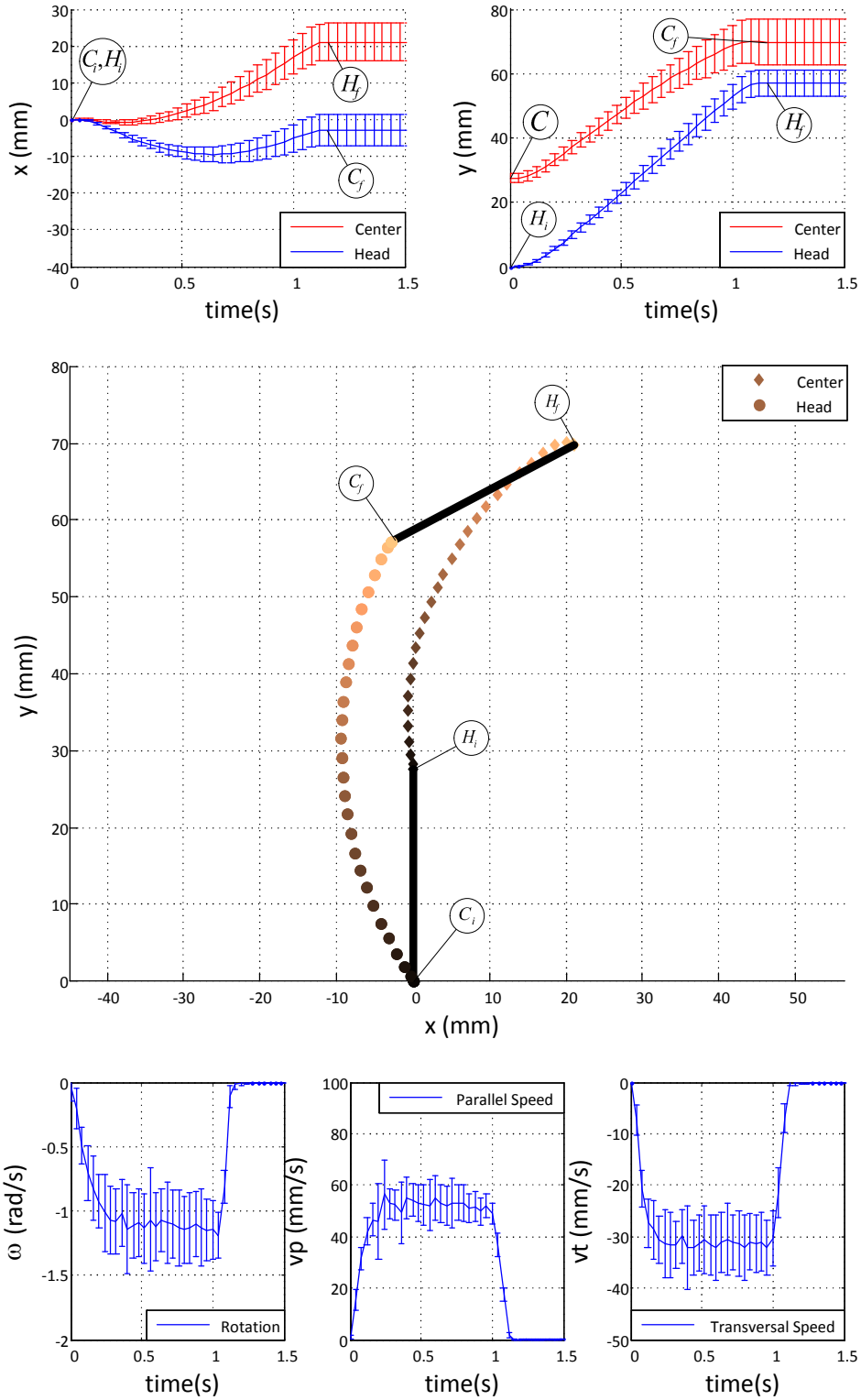

Figure 4.2 Displacement and velocity data adquired from a clockwise (CLW) motor rotation at 170 Hz for a period of 1s.

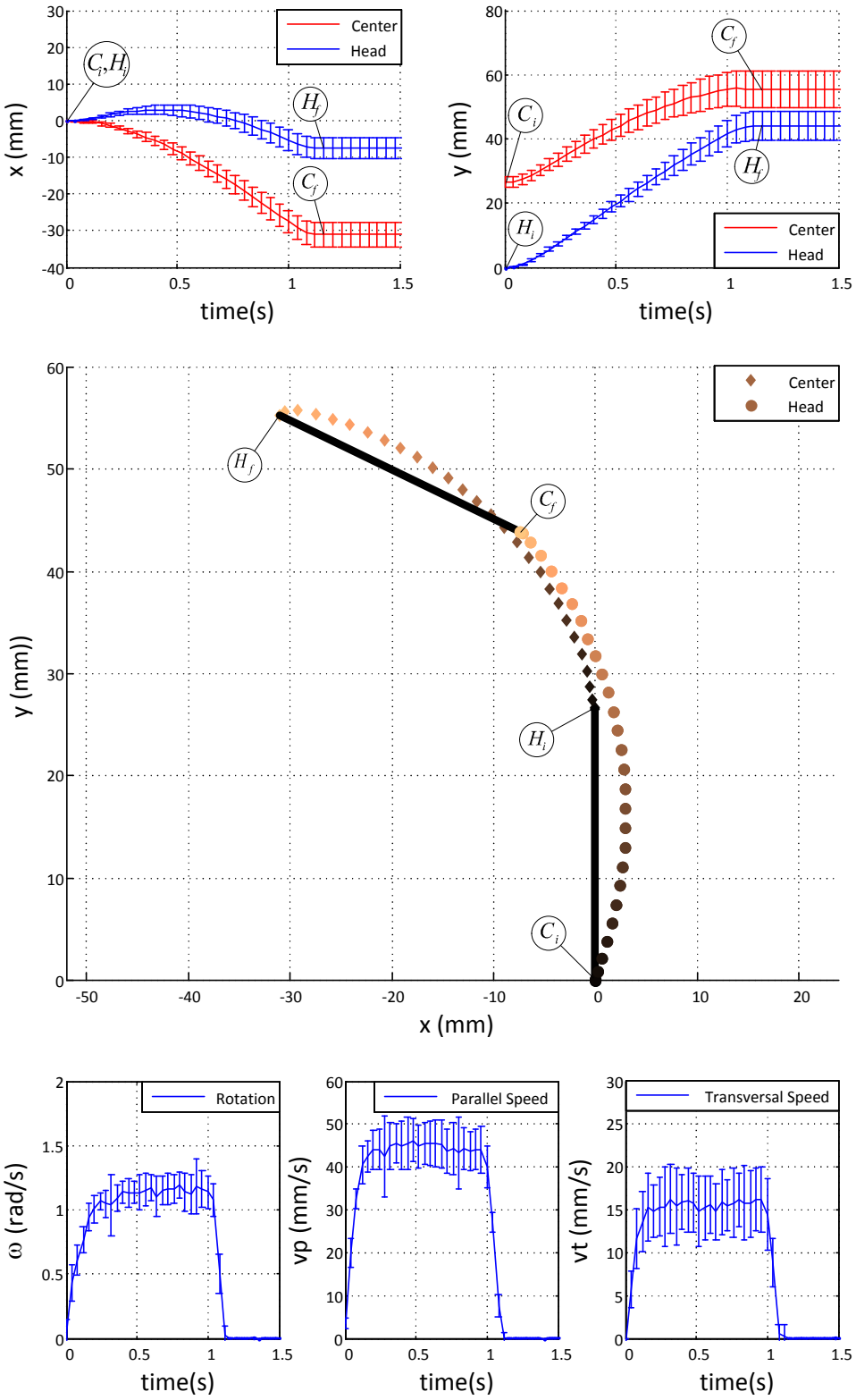

Figure 4.3 Displacement and velocity data adquired from a counter clockwise (CCW) motor rotation at 170 Hz for a period of 1s.

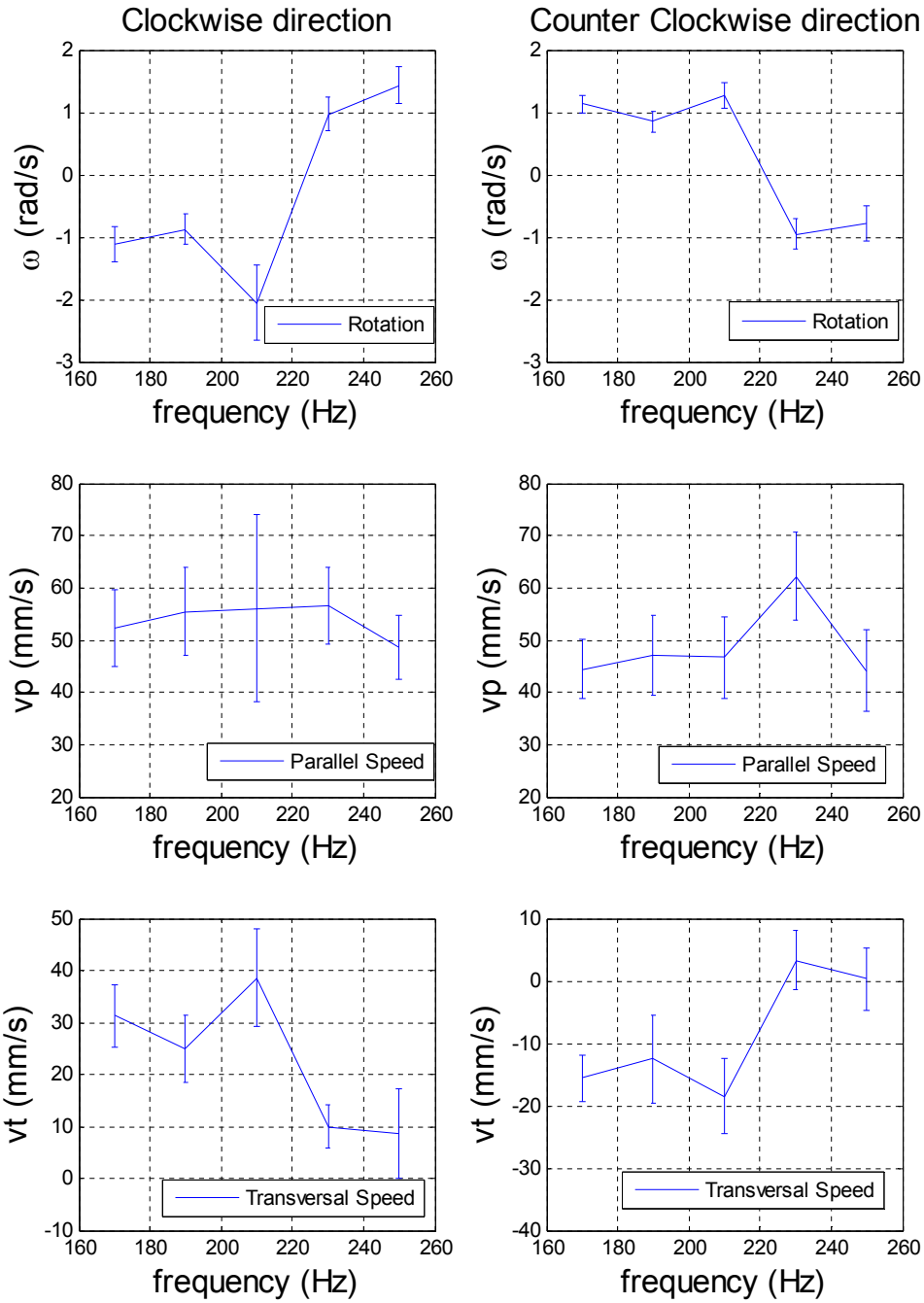

Figure 4.4 Rotation, parallel and transversal speeds of the robot at different motor rotation frequencies and direction

4.4 Discussion

It can clearly be seen in Figure 4.2 and Figure 4.3, that curved trajectories are generated in both motor directions. While the parallel velocity positive magnitude is

maintained in both cases, the rotation speed and transversal velocity have opposite directions, creating curved trajectories with opposite orientations as clearly seen in simulation results shown in Figure 2.11. In both cases, the rotation speed and parallel velocity maintain a similar magnitude, however, the transversal velocity magnitude is not equal. Instead, it is halved in the CCW direction. In both cases, all three speeds maintain a constant value after a setting time, and, decrease rapidly when the motor is shut.

In Figure 4.4, changes in the motor frequency show variance in the speeds of the robot. In Frequencies up to 210 Hz, the rotation direction of the robot is maintained while the magnitude slightly varies. However, for frequencies of 230 and 250 Hz, the rotation direction of the robot is reversed, maintaining a similar magnitude. In the CLW direction, the parallel speed is maintained around 55 mm/s for all frequencies, while in the CCW direction, a 45 mm/s is maintained whit an exception of 60 mm/s at 230 Hz. The transversal speeds values are maintained around 30 mm/s and 15 mm/s at frequencies of 170 and 210 Hz for the CLW and CCW directions, respectably. However, at frequency values of 230 and 250 Hz, both magnitudes are reduced to 10 mm/s and 1 mm/s. As it can be clearly seen, a same rotation value can be achieved with the both vibration rotations at different frequencies, however, the same movement is not developed due to the change on the transversal speed. An asymmetry between CLW and CCW is clearly seen on the speed values. This could happen, due to the manual assembly of the bristle and the mechanical chassis.

CONCLUSIONS

In this work, the design of a swarm robot agent is presented and validated with simulations and practical experiments. Its locomotion module is developed using a bristle-base exchangeable chassis driven by a single vibro-motor actuator. The electronic subsystem of the agent allows autonomous and programmed locomotion. It is comprised of an ATMEGA328P microcontroller, an infrared (IR) transmitter and two receivers for communications between agents (peer-to-peer) and sensing, an IrDA transceiver for the master host (Windows PC), a RGB transmitter for positional reference and a Li-ion battery for autonomous functioning.

A programming and control interface was developed over Visual C# on a Windows PC, and a hardware USB-IrDA adapter, to generate and transmit commands over serial transmission to an agent using a new defined protocol. Communication with the agent was successful.

Several experiments were developed to evaluate the locomotion performance of the robot; where its normal trajectory and developed speeds were analyzed. Parallel speed do not change drastically by changing the rotation frequency, however, rotation and transversal speed do change significantly in direction or magnitude, which enables locomotion in any forward direction, while lateral displacements and rotation can be controlled.

It is concluded that the developed bristle based micro-robot has the application – qualities and capacity to be used as an agent of a swarm robotic system.

FUTURE WORK

Future works should be oriented to the realization of a robotic swarm system using the developed micro-robot agent. The communication module and interaction between agents should be evaluated, and, locomotion dependent over their interactions could be developed to analyze different collective behaviors to overcome different objectives.

REFERENCES

[1] E. Garcia, M. A. Jimenez, P. Gonzalez De Santos and M. Armanda, "The evolution of robotics research," *IEEE Robotics & Automation Magazine,* vol. 14, no. 1, pp. 90-103, 2007.

[2] E. Bonabeu, M. Dorigo and G. Theraulaz, Swarm Intelligence: From Natural to Artificial Systems, New York: Oxford University Press, Inc., 1999.

[3] G. Caprari, P. Balmer, R. Piguet and R. Siegwart, "The autonomous micro robot "Alice": a platform for scientific and commercial applications," in *International Symposium on Micromechatronics and Human Science, MHS* , Nagoya, 1998.

[4] S. Fahlbusch, S. Fatikow, J. Seyfreid and A. Buerkle, "Flexible Microrobotic System MINIMAN: Design, Actuation Principle and Control," in *IEEE/ASME International Conference on Advanced Intelligent Mechatronics*, Atlanta, 1999.

[5] R. Casanova, A. Saiz-Vela, A. Arbat, J. Colomer, P. Miribel, A. Dieguez, M. Puig and J. Samitier, "Integrated Electronics for a 1cm3 Robot for Micro and Nanomanipulation Applications: MiCRoN," in *The First IEEE/RAS-EMBS International Conference on Biomedical Robotics and Biomechatronics, BioRob* , Pisa, 2006.

[6] H. Woern, M. Szymanski and J. Seyfreid, "The I-SWARM project," in *The 15th IEEE International Symposium on Robot and Human Interactive Communication, ROMAN*, Hatfield, 2006.

[7] M. Rubenstein, C. Ahler and R. Nagpal, "Kilobot: A Low Cost Scalable Robot System for Collective Behaviors," in *IEEE International Conference on Robotics and Automation*, 2012.

[8] F. Arvin, J. C. Murray, L. Shi and C. Zhang, "Development of an autonomous micro robot for swarm robotics," in *2014 IEEE International Conference on*

Mechatronics and Automation (ICMA), Tianjin, 2014.

[9] F. Becker, S. Börner, V. Lysenko, I. Zeidis and K. Zimmermann, "On the Mechanics of Bristle-Bots - Modeling, Simulation and Experiments," in *Proceedings of ISR ROBOTIK*, Munich, 2014.

[10] W. Oskay, "Bristelbot: a tiny directional vibrobot," 19 12 2007. [Online]. Available: http://www.evilmadscientist.com/2007/bristlebot-a-tiny-directional-vibrobot/. [Accessed 18 11 2015].

[11] A. Atyabi and D. M. W. Powers, "The Use of Area Extended Particle Swarm Optimization (AEPSO) in Swarm Robotics," in *11th International Conference on Control Automation Robotics & Vision (ICARCV)*, Singapore, 2010.

[12] J. Brufau, M. Puig-Vidal, J. Lopez-Sanchez, J. Samitier, N. Snis, U. Simu, S. Johansson, W. Driesen, J. Breguet, J. Gao, T. Velten, J. Seyfried, R. Estana and H. Woern, "MICRON: Small Autonomous Robot for Cell Manipulation Applications," in *IEEE International Conference on Robotics and Automation, CRA* , Barcelona, 2005.

[13] S. Kornienko, O. Kornienko and P. Levi, "Collective AI: context awareness via communication," in *Proceedings of the 19th International Joint Conference on Artificial Intelligence (IJCAI)*, Edinburg, 2005.

[14] N. Snis, "Actuators for autonomous microrobots," in *Digital Comprehensive Summaries of Uppsala Dissertations from the Faculty of Science and Technology 431*, Acta Universitatis Upsaliensis, 2008.

[15] S. Project, "Swarmanoid," 14 8 2011. [Online]. Available: http://www.swarmanoid.org/. [Accessed 15 07 2015].

[16] M. Dorigo and et al., "Swarmanoid: A Novel Concept for the Study of Heterogeneous Robotic Swarms," *IEEE Robotics & Automation Magazine,* vol. 20, no. 4, pp. 60-71, 2013.

[17] K. Ioi, “A Mobile Micro-Robot using Centrifugal Forces,” in *IEEE/ASME International Conference on Advanced Intelligent Mechatronics*, Atlanta, 1999.

[18] K. Ioi, “Study on Turning Motion of Micro Robot driven by Cyclic Force,” in *IEEE/ASME International Conference on Advanced Intelligent Mechatronics*, Como, 2001.

[19] I. F. L. Inc., “Hexbug NANO: the robotic creature that behaves like a real bug!,” [Online]. Available: https://www.hexbug.com/nano/. [Accessed 18 11 2015].

[20] V. Lysenko, K. Zimmermann, A. Chigarev and F. Becker, “A mobile vibro-robot for locomotion through pipelines,” in *56th IWK International Scientific Colloquium*, Ilmenau, 2011.

[21] F. Becker, S. Börner, T. Kästner, V. Lysenko, I. Zeidis and K. Zimmermann, “Spy Bristle Bot– A Vibration-driven Robot For The Inspection of Pipelines,” in *58th ILMENAU SCIENTIFIC COLLOQUIUM*, Ilmenau, 2014.

[22] L. Giomi, N. Hawley-Weld and L. Mahadevan, “Swarming, swirling and stasis in sequestered bristle-bots,” in *Proceedings of the Royal Society A*, 2013.

[23] A. LCC, “Arduino,” Arduino LCC, 28 02 2016. [Online]. Available: https://www.arduino.cc/.

[24] Precision Microdrives Limited, “Precision Microdrives: Vibration motor Catalog,” 2015. [Online]. Available: https://catalog.precisionmicrodrives.com/order-parts. [Accessed 07 04 2015].

[25] D. Camera, “Four Walled Cubicle,” Four Walled Cubicle, 2013. [Online]. Available: http://www.fourwalledcubicle.com/LUFA.php. [Accessed 2015].

[26] E. Teacher, “Electronics Teacher,” 2015. [Online]. Available: http://www.electronicsteacher.com/robotics/type-of-robots.php.

[27] S. Kernbach, D. Haebe, O. Kernbach, R. Thenius, G. Radspieler, T. Kimura and T. Schmickl, “Adaptative collective decision-making in limited robot swarms without communication,” *The International Journal of Robotics Research,* vol. 32, no. 1, pp. 35-55, 2013.

APPENDIX A

F. Becker[1], F. Cuellar[2], J. E. Pozo Fortunić[3], V. Lysenko[4], V. T. Minchenya[5], I. Zeidis[6], K. Zimmermann[7]

[1]Technische Universität Ilmenau, PhD Research Scientist, felix.becker@tu-ilmenau.de

[2]Pontificia Universidad Católica del Perú, Professor, cuellar.ff@pucp.edu.pe

[3]Technische Universität Ilmenau / Pontificia Universidad Católica del Perú, Master Student, edmundo.pozof@pucp.edu.pe

[4]Belarusian National Technical University, PhD Research Scientist, victor_lysenko@mail.ru

[5]Belarusian National Technical University, Professor, vlad_minch@mail.ru

[6]Technische Universität Ilmenau, PhD Research Scientist, igor.zeidis@tu-ilmenau.de

[7]Technische Universität Ilmenau, Professor, klaus.zimmermann@tu-ilmenau.de

BRISTLEBOTS IN SWARM ROBOTICS – NEW APPROACHES IN MODELING AND AGENT DEVELOPMENT

Bristlebots are vibration-driven mobile robots. They are characterized by small size, high speed, simple design and low costs of production and application, which are advantageous qualities for agents of swarm robotic systems. In this paper, new approaches in modeling and development of swarm agents are given. It is shown that a simple mass point model can be used to simulate the motion behavior of a bristlebot as complex as necessary for swarm studies. A robot prototype is presented, which has on-board everything needed as a robotic agent. The results of simulations and experiments are presented and compared.

Introduction

Swarm robotics is a recent trend in mobile robotics. It focuses on the study and development of robotic systems comprising a great number of agents that cooperate in order to fulfill tasks. Especially in the vast fields of inspection, communication and transportation technology, swarm robotic solutions can achieve admirable results. Biological examples of swarms can give an insight into the amazing potential lying in the cooperation of individuals [1]. Inspired by insects that live in colonies, researches try to create miniaturized artificial swarm robotic systems [2 - 8]. For this reason, simple, small and light hardware platforms with low power consumption are needed. An important part of a mobile robot is its locomotion module. It creates actuation forces to accelerate the robot. Locomotion modules based on bristlebots are simple and reliable solutions [7 - 13].

The locomotion of bristlebots is driven by the vibration of internal masses. The periodic excitation is transformed into directed motion due to asymmetric friction properties achieved by bristles. The working principle can be divided into two groups – 1st: short, stiff bristles or spikes which can mechanically interlock with a surface; and – 2nd: long, elastic bristles which can be deformed and create the asymmetric friction properties caused by periodic normal forces. Both different locomotion schemes are studied in detail in [9].

To the authors, the first publication concerning bristlebots is known in the youth journal "Юный Техник" in 1977 [14]. A bristlebot with the ability to find light sources autonomously was presented in the same journal one year later [15]. Bristlebots have its renaissance over the last ten years, e. g. as self-made toys constructed from a tooth brush, a button cell battery and a vibration motor form a cell phone or pager. The idea to use bristlebots in microrobot teams is presented in [7], [8]. The robots in [8] are not equipped with additional electronics like it is usual for swarm robots. The only form of swarm intelligence, communication or interaction between the individuals is the mechanical interaction due to collisions with borders of a test area and between the robots. Swarm behavior can be observed, if the number of robots per area exceeds a critical amount.

The aim of this paper is to give approaches to modeling and agent development in swarm robotics. The presented robot prototype is based on bristlebots – a simple, robust and cheap locomotion technology. The proposed model comprises the main influences from geometry and motor control to the two-dimensional locomotion system and may be used as basis for complex simulations of homogenous or heterogeneous swarms with bristlebot-based agents.

Mechanical model and equations of motion

For swarm simulations the underlying mechanical model of an agent should be as simple as possible, but should comprise the dominant locomotion mechanisms. Analyses of the motion behavior of bristlebots in [9 - 12] show that the locomotion is determined by periodic actuation forces and non-symmetric friction forces. The proposed mass point model is presented in Fig. 1.

The system is composed by two mass points P_1 and P_2, which carry masses m_1 and m_2, respectively. They are connected by a massless bar of the length $\overline{CP_1}+\overline{CP_2}=b_1+b_2$. Two Cartesian coordinate systems are introduced: a fixed reference frame with the unit vectors $\left(\vec{e}_x,\vec{e}_y,\vec{e}_z\right)$, and a body-attached frame with $\left(\vec{E}_x,\vec{E}_y,\vec{E}_z\right)$, which is situated in the center of mass $C(x_c,y_c,z_c)$. The motion of the system is limited to the plane $\left(\vec{e}_x,\vec{e}_y\right)$, therefore $\vec{e}_z=\vec{E}_z$. The number of degrees of freedom equals three. With the angle $\angle(\vec{e}_x,\vec{E}_x)=\theta$, it follows

$$\begin{aligned} \vec{e}_x &= cos\,\theta\vec{E}_x - sin\,\theta\vec{E}_y, & \vec{E}_x &= cos\,\theta\vec{e}_x + sin\,\theta\vec{e}_y, \\ \vec{e}_y &= sin\,\theta\vec{E}_x + cos\,\theta\vec{E}_y, & \vec{E}_y &= -sin\,\theta\vec{e}_x + cos\,\theta\vec{e}_y. \end{aligned} \tag{1}$$

The vibration motor generates the forces $\vec{A}_y$ and $\vec{A}_z$ at the point A. They are determined by the motion of the mass m_e on a circular orbit with a radius e and angular velocity $\dot{\varphi}=\Omega$ in the plane $\left(\vec{E}_y,\vec{E}_z\right)$:

$$\begin{aligned} \vec{A}_y &= -m_e e\Omega^2\, cos\left(\Omega t\right)\vec{E}_y, \\ \vec{A}_z &= -\left[m_e g - m_e e\Omega^2\, sin\left(\Omega t\right)\right]\vec{E}_z. \end{aligned} \tag{2}$$

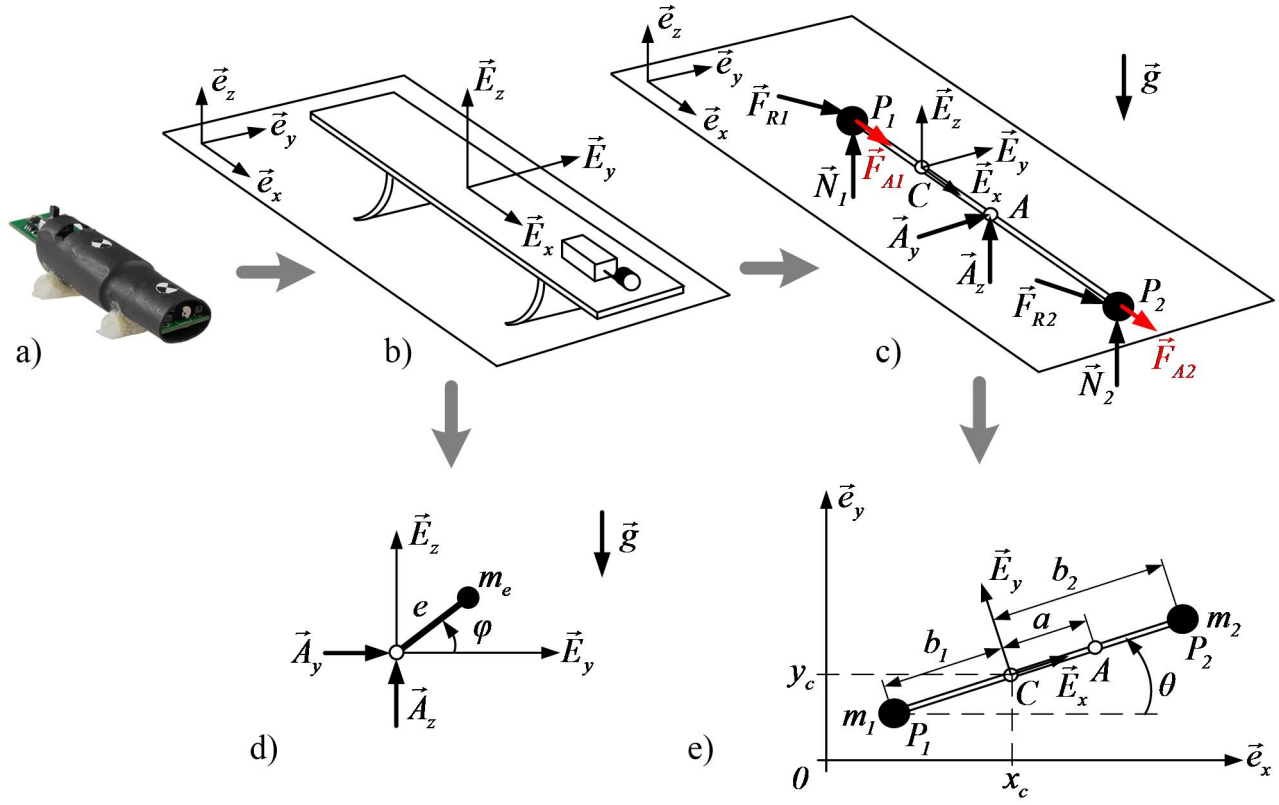

a) Robot prototype; b) Schematic robot; c) Robot model with forces; d) Motor model; e) Geometry and coordinates

Fig. 1. Modeling of the robot

At the points P_1 and P_2, normal forces $\vec{N}_1, \vec{N}_2$, Coulomb dry friction forces $\vec{F}_{R1}, \vec{F}_{R2}$ and actuation forces $\vec{F}_{A1}, \vec{F}_{A2}$ are applied. The actuation forces are modeling the periodic forward forces produced by the elastic bristles due to the excitation of the motor:

$$\vec{F}_{A1} = F_{A1} \sin(\Omega t)\, \vec{E}_x, \qquad \vec{F}_{A2} = F_{A2} \sin(\Omega t)\, \vec{E}_x. \tag{3}$$

As the actuation forces of bristles are developed by the frictional contact between the robot and ground, their magnitudes F_{A1} and F_{A2} may not exceed the friction forces in backward direction. The normal forces $\vec{N}_1 = N_1 \vec{E}_z$ and $\vec{N}_2 = N_2 \vec{E}_z$ can be calculated using the equilibrium of forces in $\vec{e}_z$-direction and the equilibrium of moments about $\vec{E}_y$:

$$\begin{aligned} 0 &= N_1 + N_2 + A_z - (m_1 + m_2) g, \\ 0 &= -b_1 N_1 + b_2 N_2 + a A_z. \end{aligned} \tag{4}$$

With $\overline{CA} = a$, it follows:

$$\begin{aligned} N_1 &= \frac{b_2}{b_1 + b_2} (m_1 + m_2) g + \frac{b_2 - a}{b_1 + b_2} \left[m_e g + m_e e \Omega^2 \sin(\Omega t) \right] \\ N_2 &= \frac{b_1}{b_1 + b_2} (m_1 + m_2) g + \frac{b_1 + a}{b_1 + b_2} \left[m_e g + m_e e \Omega^2 \sin(\Omega t) \right]. \end{aligned} \tag{5}$$

In order to fulfill the condition of constant contact, it is needed that $N_1 \geq 0$ and $N_2 \geq 0$. To obtain the friction forces

$$\vec{F}_{R1} = -\mu |N_1| \frac{\dot{\vec{r}}_1}{|\dot{\vec{r}}_1|}, \qquad \vec{F}_{R2} = -\mu |N_2| \frac{\dot{\vec{r}}_2}{|\dot{\vec{r}}_2|}, \tag{6}$$

the velocities of P_1 and P_2 are determined:

$$\begin{aligned} \dot{\vec{r}}_1 &= \dot{x}_1 \vec{e}_x + \dot{y}_1 \vec{e}_y = \left(\dot{x}_c + b_1 \dot{\theta} \sin\theta\right)\vec{e}_x + \left(\dot{y}_c - b_1 \dot{\theta} \cos\theta\right)\vec{e}_y, \\ \dot{\vec{r}}_2 &= \dot{x}_2 \vec{e}_x + \dot{y}_2 \vec{e}_y = \left(\dot{x}_c - b_2 \dot{\theta} \sin\theta\right)\vec{e}_x + \left(\dot{y}_c + b_2 \dot{\theta} \cos\theta\right)\vec{e}_y. \end{aligned} \tag{7}$$

Absolute values of the velocities are $|\dot{\vec{r}}_1| = \sqrt{(\dot{x}_1)^2 + (\dot{y}_1)^2} \neq 0$ and $|\dot{\vec{r}}_2| = \sqrt{(\dot{x}_2)^2 + (\dot{y}_2)^2} \neq 0$. The principle of linear momentum $M\ddot{\vec{r}} = \sum \vec{F}$, where $M = m_1 + m_2 + m_e$ and $\ddot{\vec{r}} = \ddot{x}_c \vec{e}_x + \ddot{y}_c \vec{e}_y$, can be written in two scalar equations on the fixed reference frame $(\vec{e}_x, \vec{e}_y, \vec{e}_z)$:

$$M\,\ddot{x}_c = -\mu |N_1| \frac{\dot{x}_1}{|\dot{\vec{r}}_1|} - \mu |N_2| \frac{\dot{x}_2}{|\dot{\vec{r}}_2|} + m_e e \Omega^2 \cos(\Omega t) \sin\theta + (F_{A1} + F_{A2}) \sin(\Omega t) \cos\theta, \tag{8}$$

$$M\,\ddot{y}_c = -\mu |N_1| \frac{\dot{y}_1}{|\dot{\vec{r}}_1|} - \mu |N_2| \frac{\dot{y}_2}{|\dot{\vec{r}}_2|} - m_e e \Omega^2 \cos(\Omega t) \cos\theta + (F_{A1} + F_{A2}) \sin(\Omega t) \sin\theta. \tag{9}$$

The principle of angular momentum $\dot{\vec{D}}_C = \sum \vec{M}_C$ is applied in the center of mass C with $J = m_1 b_1^2 + m_2 b_2^2 + m_e a^2$ and $\dot{\vec{D}}_C = J\ddot{\theta}\vec{E}_z$:

$$J\ddot{\theta} = -a\, m_e e \Omega^2 \cos(\Omega t) - b_1 \mu |N_1| \frac{1}{|\dot{\vec{r}}_1|} (\dot{x}_1 \sin\theta - \dot{y}_1 \cos\theta) - b_2 \mu |N_2| \frac{1}{|\dot{\vec{r}}_2|} (\dot{x}_2 \sin\theta - \dot{y}_2 \cos\theta). \tag{10}$$

Simulation

To analyze the presented model, the equations of motion are numerically integrated in MATLAB/Simulink. The values of the parameters, which refer to the prototype presented in Fig. 1, are given in Table 1. It should be mentioned that the parameter range is limited by the condition of constant contact: $N_1 \geq 0$ and $N_2 \geq 0$ discussed previously. Some results of the simulations are presented in Fig. 2. It shows trajectories of the points P_1, P_2 and C for different values of parameters. It may be seen that the robot model moves on a curved orbit. The radius of the trajectory and the velocity depend on the rotational speed of the motor Ω. The turning direction of the model can be controlled by the sign of Ω. The position of the mass m_e relative to the center of mass C of the overall system is labeled with a. The influence of a to the orbit due to the produced torque is also presented in Fig. 2. It is obvious that the increasing overall mass $M = m_1 + m_2 + m_e$ reduces the velocity. Moreover, the system moves faster for a small friction coefficient μ.

Table 1. Model parameters used in the simulations

Model geometry	b_1	15 mm	b_2	15 mm	a	33 mm
Mass distribution	m_1	5 g	m_2	5 g	J	2.5 kg mm²
Motor parameters	m_e	0.3 g	e	0.2 mm	Ω	-6000 rpm
Environment	g	9.81 m/s²	μ	0.05	t	0 .. 10 s
Actuation forces	F_{A1}	0.0624 N	F_{A2}	0.0624 N		

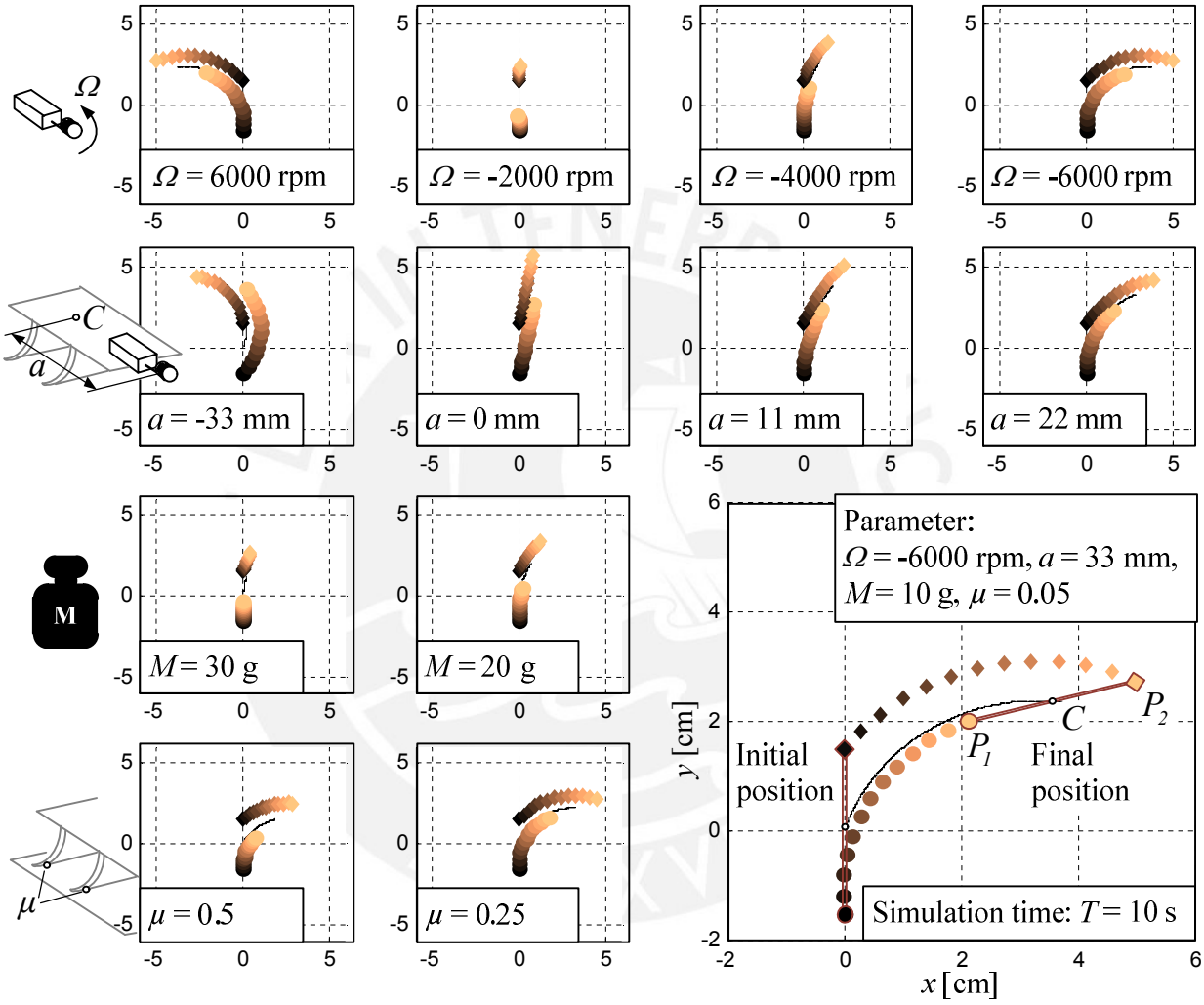

Fig. 2. Numerical parameter study: trajectories of the points P_1, P_2 and C for different values of parameters

Prototype

The developed swarm argent prototype is presented in Fig. 3. It is a bristlebot equipped with additional electronics for programming, autonomous locomotion and communication. From the mechanical point of view, the robot consists of a rigid main body with a total mass M = 10 g, an internal rotating mass point m_e = 0.3 g and two rows of elastic bristles made from foam plastics. The rows are attached to an exchangeable chassis which allows the use of bristle systems with different characteristics. Two markers on the chassis are needed for the optical motion tracking and could be used for automatic locomotion control. The electronic system of the robot consists of a

conductor board, an actuation system (motor and motor driver), a power management (battery, voltage regulators), a communication and sensing system (upward and peer-to-peer communication) and a microprocessor.

An Atmega328P microprocessor is used. It has sufficient resources and peripherals to control the system. Due to its application in the well-known Arduino boards, the system can be programmed and expanded over Arduino sketch file programming. The DC vibration motor is controlled using an H-bridge for the rotation direction and pulse-width modulation for the value of angular speed. A Li-ion battery is used with a capacity of 100 mAh. For the communication with the master host (Windows PC), the IrDA technology is selected due to its price, robustness and simplicity. Custom infrared (IR) is used for the communication between the agents (peer-to-peer). The IR wavelength bandwidth does not interfere with the IrDA spectrum. Each agent will have an IR transmitter on the back and two IR receivers at the front. It can be used for different tasks, e. g. following a trail or finding IR sources. Similar to the chemical "leaving a trail"-methods of ants, the robot agents can follow each other.

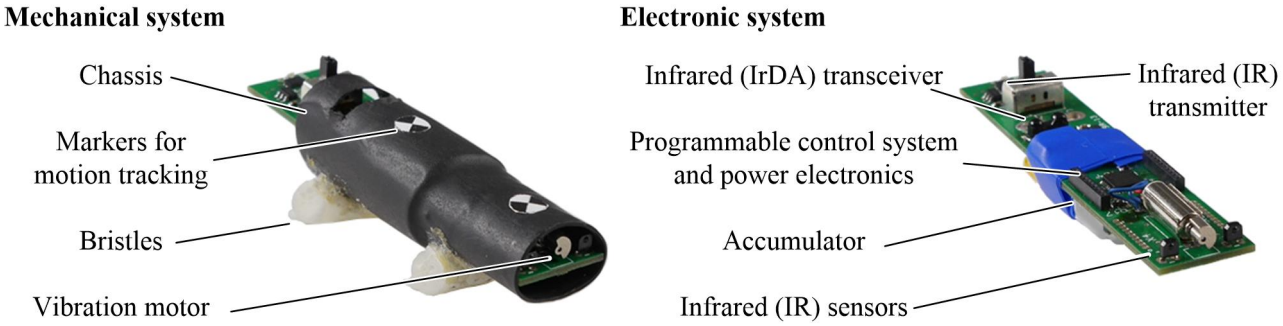

a) Mechanical system; b) Electronic system

Fig. 3. Prototype of a bristlebot swarm agent

Experiments on locomotion

The experiments on locomotion are performed tracking the markers on a video. Depending on the rotation direction and speed of the motor, different trajectories are observed. Fig. 4 presents motion trajectories of the prototype for different rotational speeds and signs of rotation. The mean value of ten repetitions of the experiments and the root mean square deviation of the measured final position are plotted. As predicted by the simulations, the robot moves always on a curved orbit. By increasing the motor speed, the prototype can move faster and the radius of the trajectory decreases. Of special interest that the motion direction of the robot inverts for high rotational speed ($\Omega > 12000$ rpm) due to resonance effects. As stated in [16] and [17], resonance behavior can be used to control the motion direction of vibration-driven locomotion systems by the excitation frequency.

Using the electronic control system, the robot's way in the *xy*-plane can be combined from a number of curved orbits.

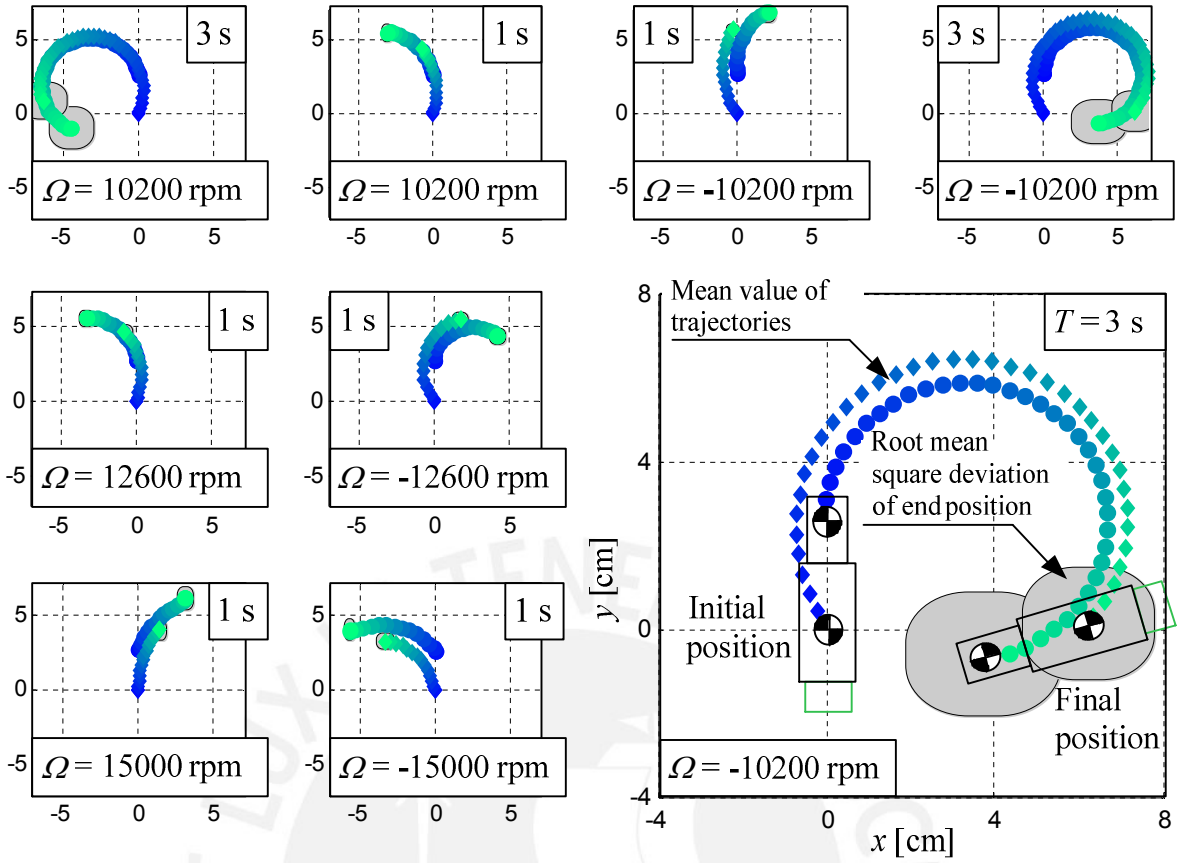

Fig. 4. Experimental parameter study: trajectories of the markers for different rotation speeds Ω and motion times T

Conclusions and outlook

In this paper, a swarm robot agent is presented. The system is inspired by bristlebots. The locomotion can be controlled by rotational speed and rotation direction of the vibration motor. The electronic system of the agent allows autonomous and programmed locomotion. Equipped with a microprocessor, IR receivers and an IR transmitter, it is prepared for an agent-to-agent communication which can be used to achieve swarm behavior. Furthermore, a mechanical model of a single robot is presented. Numerical examples show that it can be used to simulate the locomotion of swarm agents like presented. Due to its simplicity, it has the potential to be used as a subsystem for swarm models. The future work should be connected with the realization of a robotic swarm based on the agent. The proposed model can be used as a basis for complex swarm simulation.

Acknowledgements

This research was partly supported by Deutsche Forschungsgemeinschaft Grant ZI 540/19-1 and the PUCP Marco Polo Fund 2015-1.

References

1. Bonabeu, E. Swarm Intelligence: From Natural to Artificial Systems / E. Bonabeu, M. Dorigo, G. Theraulaz // New York: Oxford University Press, Inc. 1999.

2. Fahlbusch, S. Flexible Microrobotic System MINIMAN: Design, Actuation Principle and Control / S. Fahlbusch, S. Fatikow, J. Seyfreid, A. Buerkle, Proceedings of IEEE/ASME AIM. 1999. P. 156 – 161.

3. Casanova, R. Integrated Electronics for a 1cm3 Robot for Micro and Nanomanipulation Applications: MiCRoN / R. Casanova, A. Saiz-Vela, A. Arbat, J. Colomer, P. Miribel, A. Dieguez, M. Puig, J. Samitier // Proceedings of IEEE/RAS BioRob. 2006. P. 13 – 18.

4. Woern, H. The I-SWARM project / H. Woern, M. Szymanski, J. Seyfreid // Proceedings of IEEE RO-MAN. 2006. P. 492 – 496.

5. Rubenstein, M. Kilobot: A Low Cost Robot with Scalable Operations Designed for Collective Behaviors/ M. Rubenstein, C. Ahler, N. Hoff, A. Cabrera, R. Nagpal // Robotics and Autonomous Systems. 2014. № 62 (2). P. 966 – 975.

6. Arvin, F. Development of an autonomous micro robot for swarm robotics / F. Arvin, J. C. Murray, L. Shi, C. Zhang // Proceedings of IEEE ICMA. 2014. P. 635 – 640.

7. Christensen, D. L. Let's All Pull Together: Principles for Sharing Large Loads in Microrobot Teams / D. L. Christensen, S. A. Suresh, K. Hahm, M. R. Cutkosky // IEEE Robotics and Automation Letters. 2016. №. 1 (2). P. 1089 – 1096

8. Giomi, L. Swarming, swirling and stasis in sequestered bristle-bots / L. Giomi, N. Hawley-Weld, L. Mahadevan // Proceedings of the Royal Society A. 2013. № 469. P. 1 – 21.

9. Becker, F. On the Mechanics of Bristle-Bots - Modeling, Simulation and Experiments / F. Becker, S. Börner, V. Lysenko, I. Zeidis, K. Zimmermann // Proceedings of ISR/ROBOTIK. 2014. P. 15 – 20.

10. Ioi, K. A Mobile Micro-Robot using Centrifugal Forces / K. Ioi // Proceedings of IEEE/ASME AIM. 1999. P. 736 – 741.

11. Becker, F. Spy Bristle Bot - A Vibration-driven Robot For The Inspection of Pipelines / F. Becker, S. Börner, T. Kästner, V. Lysenko, I. Zeidis, K. Zimmermann // Proceedings of 58th IWK Ilmenau. 2014.

12. Majewski, T. Behavior of the Robot with Vibratory Excitation / T. Majewski, D. Szwedowicz // Proc. of MUSME. 2015. Mechanisms and Machine Science. № 25. P. 67 – 74

13. Han, Y. Fiberbot: A Miniature Crawling Robot Using a Directional Fibrillar Pad / Y. Han, H. Marvi, M. Sitti // Proceedings of IEEE ICRA. 2015. P. 3122 – 3127

14. Сенюткин, А. Виброходы / А. Сенюткин // Юный Техник. 1977. № 6. P. 65 – 67

15. Борисов, Ю. Виброход идёт на свет / Ю. Борисов // Юный Техник. 1978. № 4. P. 72 – 73

16. Zimmermann, K. Mechanics of Terrestrial Locomotion / K. Zimmermann, I. Zeidis, C. Behn // Springer. Berlin. 2009.

17. Becker, F. Zur Mechanik vibrationsgetriebener Roboter für terrestrische und aquatische Lokomotion / F. Becker // Phd thesis. Universitätsverlag Ilmenau. 2015.